

NO_x emissions reduction and rebound in China due to the COVID-19 crisis

Jieying Ding¹, Ronald J. van der A², Henk Eskes³, Bas Mijling¹, Trissevgeni Stavrakou⁴, Jos van Geffen⁵, and Pepijn Veeffkind³

¹KNMI Royal Netherlands Meteorological Institute

²KNMI

³Royal Netherlands Meteorological Institute

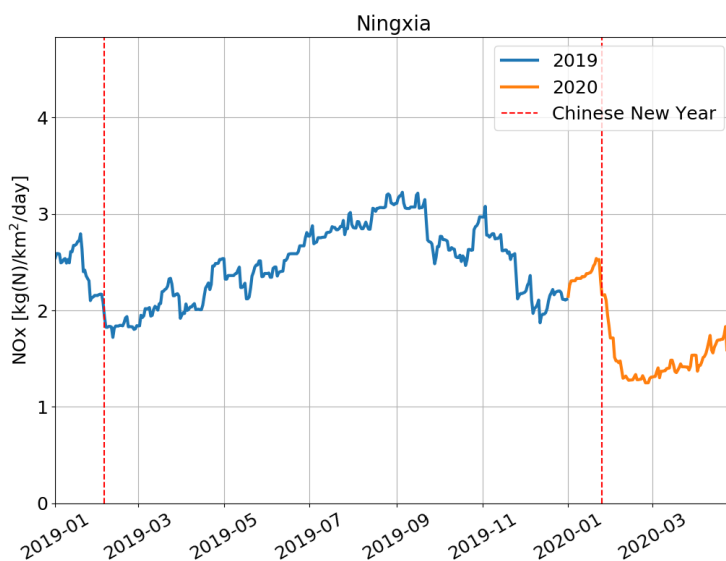
⁴Royal Belgian Institute for Space Aeronomy

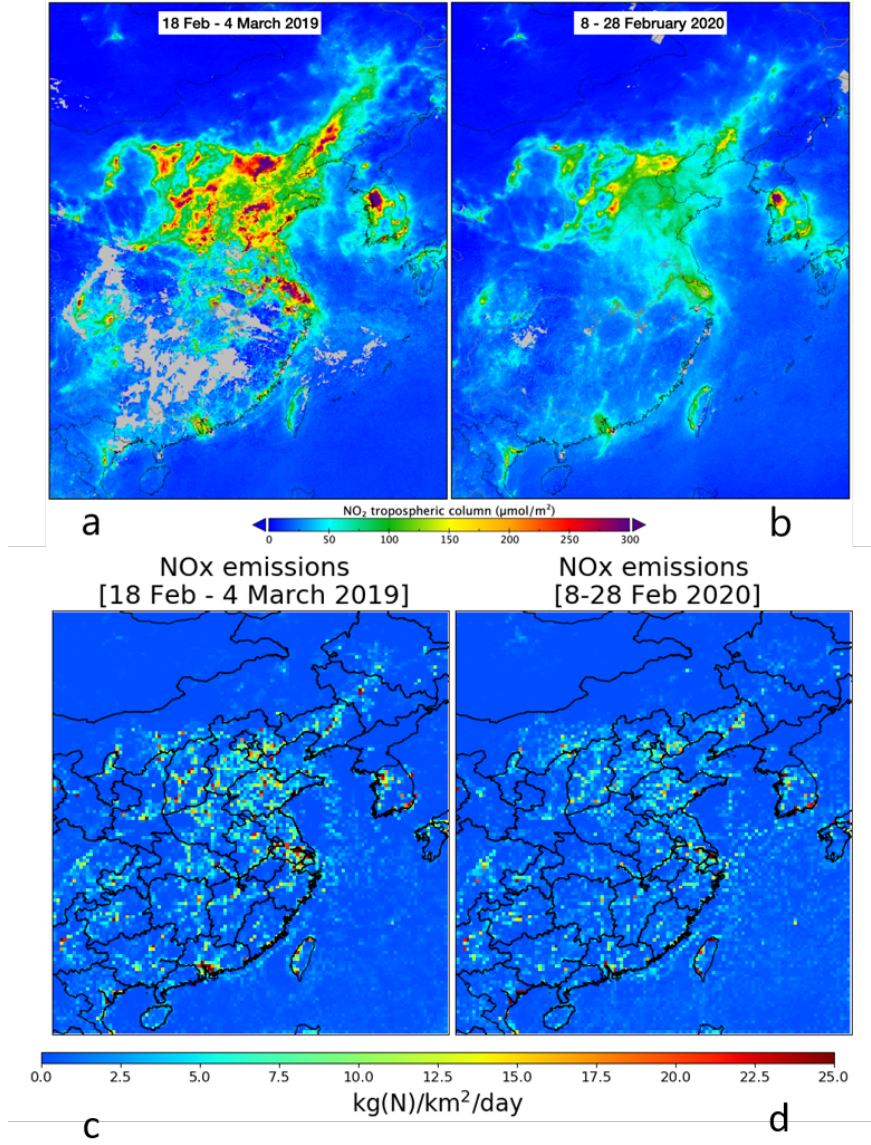
⁵Royal Netherlands Meteorological Institute, De Bilt, Netherlands

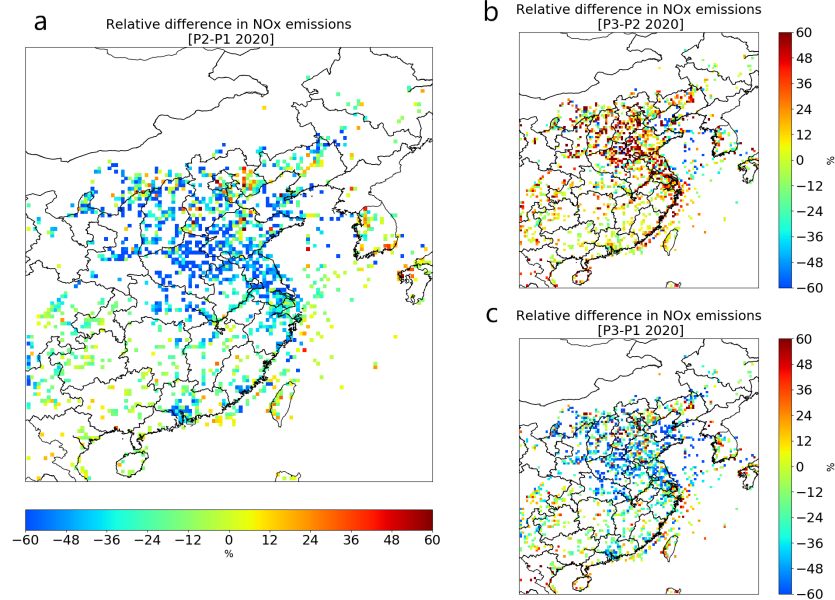
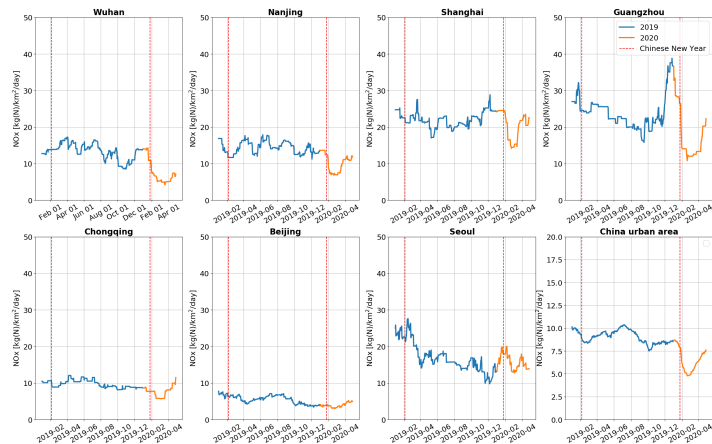
November 21, 2022

Abstract

During the COVID-19 lockdown (24 Jan to 20 March) in China low air pollution levels were reported in the media as a consequence of reduced economic and social activities. Quantification of the pollution reduction is not straightforward due to effects of transport, meteorology, and chemistry. We have analysed the NO emission reductions calculated with an inverse algorithm applied to daily NO observations from TROPOMI onboard the Copernicus Sentinel-5P satellite. This method allows the quantification of emission reductions per city, and the analysis of emissions of maritime transport and of the energy sector separately. The reductions we found are 20 to 50% for cities, about 40% for power plants and 15 to 40% for maritime transport depending on the region. The reduction in both emissions and concentrations shows a similar timeline consisting of a sharp reduction (34 to 50%) around the Spring festival and a slow recovery from mid-February to mid-March.







1
2
3
4
5
6
7
8
9
10
11
12
13
14
15
16
17
18
19
20
21

NO_x emissions reduction and rebound in China due to the COVID-19 crisis

J.Ding¹, R.J. van der A^{1,2}, H.J. Eskes¹, B. Mijling¹, T. Stavrou³, J.H.G.M. van Geffen¹, J.P. Veefkind^{1,4}

¹ Royal Netherlands Meteorological Institute (KNMI), Utrechtseweg 297, 3731 GA De Bilt, The Netherlands.

² Nanjing University of Information Science & Technology (NUIST), Ningliu Road 219, Nanjing, P.R. China.

³ Royal Belgian Institute for Space Aeronomy (BIRA-IASB), Avenue Circulaire 3, 1180 Brussels, Belgium.

⁴ Delft University of Technology, Stevinweg 1, 2628 CN Delft, The Netherlands

Corresponding author: Jieying Ding (jieying.ding@knmi.nl)

Key Points:

- NO_x emissions derived from TROPOMI observations show reductions for individual Chinese cities of about 35% due to the COVID-19 lockdown.
- Emissions of coal power plants and maritime transport show strong reductions (25-40%) during the lockdown.
- Urban emissions rebound in March to levels before the lockdown, while emissions of power plants and maritime transport take longer to recover.

22 **Abstract**

23 During the COVID-19 lockdown (24 Jan to 20 March) in China low air pollution levels were
24 reported in the media as a consequence of reduced economic and social activities. Quantification
25 of the pollution reduction is not straightforward due to effects of transport, meteorology, and
26 chemistry. We have analysed the NO_x emission reductions calculated with an inverse algorithm
27 applied to daily NO_2 observations from TROPOMI onboard the Copernicus Sentinel-5P satellite.
28 This method allows the quantification of emission reductions per city, and the analysis of
29 emissions of maritime transport and of the energy sector separately. The reductions we found are
30 20 to 50% for cities, about 40% for power plants and 15 to 40% for maritime transport
31 depending on the region. The reduction in both emissions and concentrations shows a similar
32 timeline consisting of a sharp reduction (34 to 50%) around the Spring festival and a slow
33 recovery from mid-February to mid-March.

34

35 **Plain Language Summary**

36 During the COVID-19 lockdown in China, air quality had strongly improved. Here we study
37 what sources were reduced and how much the reduction per city was. We used TROPOMI
38 observations of the Sentinel-5P satellite, which monitors the Earth's atmosphere daily. We
39 focused on observations of the pollutant 'nitrogen dioxide', an important pre-cursor of air
40 pollution in the atmosphere. With our novel methodology we are able to calculate the pollution
41 back to the sources of the emissions, whether these are big cities, industrial regions, power plants
42 or busy shipping lanes. We applied this method to East China, where the 36 biggest Chinese
43 cities are located. Almost all those cities showed strong emission reductions of 20-50% during
44 the lockdown in February 2020. Besides urban China, we found an average emission reduction
45 of 40% over coal power plants, and a reduction in maritime transport by 15-40% depending on
46 the region. The period of reduced emissions lasted until around the end of February and the
47 emissions slowly returned to normal during the month March 2020. Exception is the region
48 Wuhan, the centre of the COVID-19 crisis, where emissions started to rebound since 8 April, the
49 end of their lockdown period.

50

51 **1 Introduction**

52 The year 2020 is an unprecedented year, with the novel coronavirus, causing the COVID-
53 19 disease spreading over the whole world, infecting millions of people and causing hundreds of
54 thousands of fatalities (WHO, 2020). On 11 March 2020, the World Health Organization (WHO)
55 qualified the spread of COVID-19 as a pandemic. To prevent the spread of the disease, many
56 affected countries implemented COVID-19 regulations. China, the first country facing the
57 outbreak of COVID-19, enacted a lockdown from 24 January to 20 March 2020 in the Hubei
58 province where the first cases were reported from its capital Wuhan, while other provinces
59 limited all outdoor activities since the Chinese New Year and gradually resumed the work after
60 10 February (Tian et al., 2020; Wang et al., 2020).

61 The strict COVID-19 regulations lead to a reduction of road and air traffic, a temporary
62 closing of companies and a decrease of industrial productivity. These in consequence affect
63 emissions of air pollutants, especially from the transport and industry sectors, which are
64 significant sources of NO_x ($\text{NO}_x = \text{NO}_2 + \text{NO}$) in cities. Several studies presented a large decrease

65 of NO₂ concentration during the lockdown period in China from both in-situ and satellite
66 observations (Wang et al., 2020; Huang et al., 2020). Tropospheric NO₂ column concentrations
67 observed by the TROPOMI (TROPOspheric Monitoring Instrument) on the Sentinel-5P satellite
68 decrease about 35% over China and some areas up to 60% during the COVID-19 regulation
69 period compared to the same period of 2019 (Bauwens et al, 2020; Zhang et al., 2020; Liu et al.,
70 2020). In March 2020, after the resumption of work and the gradual lifting of the lockdown
71 restrictions, the NO₂ concentrations quickly increased to similar levels as in the previous year
72 (Bauwens et al., 2020). Because NO₂ concentrations are affected by meteorology, chemistry and
73 transport, large concentration variations are expected from day to day. Therefore the
74 concentrations alone provide only an indication of the impact of the COVID-19 measures on air
75 pollution. Bottom-up inventories are usually updated with few years delay due to the complexity
76 of gathering all statistic information on source sector, land-use and sector-specific emission
77 factors. A top-down approach using satellite observations has been demonstrated to be able to
78 accurately and quickly provide emission estimates (Stavrakou et al., 2013; Miyazaki et al. 2020).
79 Here we derived the NO_x emissions by using the satellite observations and a chemistry-transport
80 model (CTM). The model is driven by meteorological analyses, accounting for the weather-
81 related variability. The high spatial resolution of the TROPOMI observations and the inverse
82 modelling system allows us to quantify the impact of the COVID-19 measures and distinguish
83 emissions from cities, power plants and maritime transport separately. Recently, NO_x emissions
84 derived from the high resolution NO₂ observations of TROPOMI have been reported by
85 Goldberg et al. (2019) and van der A et al. (2020).

86 To this purpose, we use the DECSO (Daily Emission estimates Constrained by Satellite
87 Observations) algorithm, which has been demonstrated to capture emission changes in a short
88 time period at city level (Mijling and van der A, 2012; Ding et al., 2015). This study presents
89 NO_x emissions estimated from Sentinel-5P TROPOMI observations from 2019 to April 2020
90 over East Asia. The high spatial resolution satellite observations and daily global coverage allow
91 us to monitor fast emission changes per city due to the implementation and to the relaxing of
92 COVID-19 regulations.

93

94 **2 Methodology**

95

96 **2.1 NO₂ observations by TROPOMI**

97 The Copernicus Sentinel-5P satellite carries the TROPOMI instrument (Veefkind et al,
98 2012). TROPOMI is a spectrometer combining a high spectral resolution with high spatial
99 resolution (3.5 x 5.5 km² at nadir for the NO₂ observations), low noise and a daily global
100 coverage. Despite the much smaller footprints, the spectral fits of the individual TROPOMI
101 ground pixels have 30% smaller noise than those from the earlier Ozone Monitoring Instrument
102 (OMI) and the average values agree well within 5% (van Geffen et al, 2020).

103 Validation studies (Judd et al, 2020; Tack et al, 2020; Verhoelst et al, 2020) show that
104 the currently available TROPOMI product (versions 1.2.2 and 1.3.0) has tropospheric columns
105 with effectively a typical systematic bias of about -15% (see Supplementary Information), and
106 we expect the derived emissions from these observations to be low by such an amount on

107 average. In the relative comparisons discussed in this paper for both columns and emissions we
108 expect a large part of such a multiplicative bias to cancel out.

109 Figure 1 (a and b) shows the mean TROPOMI NO₂ tropospheric column observations
110 gridded on a 0.02° by 0.02° grid for the periods 8-28 February 2020 compared with 18 February
111 to 4 March 2019, both after the Chinese New Year holidays. Very prominent concentration
112 reductions are observed in 2020 compared to 2019.

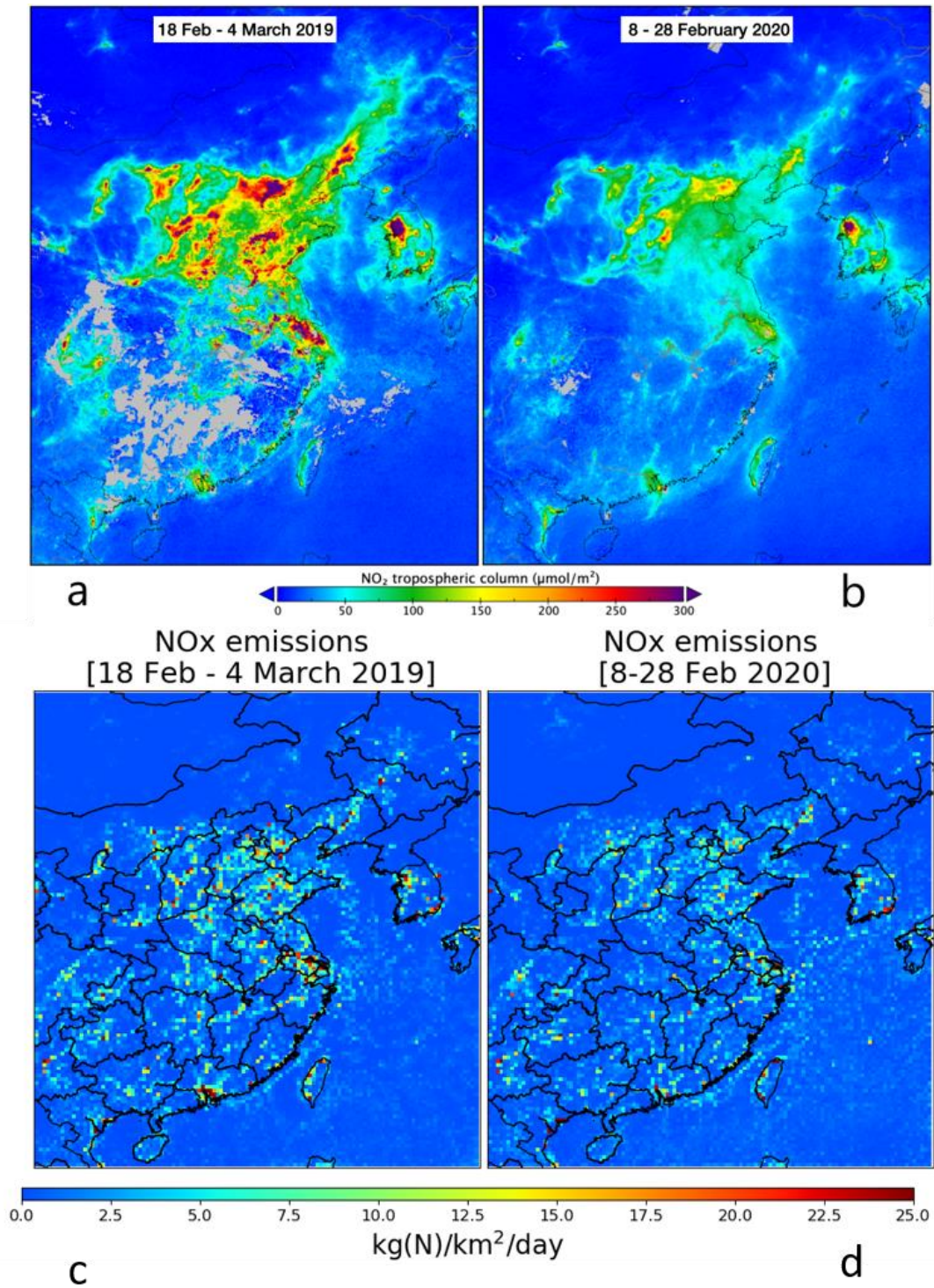
113 The TROPOMI tropospheric NO₂ columns are pre-processed into “super-observations”,
114 representing the integrated average of the TROPOMI observations over the 0.25° x 0.25° grid
115 cells of the model after filtering for clouds. The basic concept of super-observations has been
116 explained in Myazaki et al. (2012) and Boersma et al. (2016). They have shown that clustering
117 individual observations into super-observations has a positive impact on the analysis. The super-
118 observation error takes into account spatial correlations between individual TROPOMI
119 observations as well as representativity errors in the case of incomplete coverage. Averaging
120 kernels are also computed for these super-observations, and are used in the emission estimates
121 described below. This has the advantage that the inversion result becomes independent of the
122 coarser-resolution of the a priori profile used in the retrieval of the tropospheric column.

123

124

125

126



127

128 **Figure 1.** TROPOMI NO₂ columns over East China after the Chinese New Year in 2019 (a) and
129 2020 (b). NO_x emissions for the same period in 2019 (c) and 2020 (d) derived with DECSO.

130

131

132 2.2 NO_x emissions from DECSO

133 DECSO is a state-of-the-art inverse algorithm developed by Mijling and van der A
134 (2012) to update daily emissions of short-lived atmospheric constituents using an extended
135 Kalman filter, in which emissions are translated to concentrations via a CTM and compared to
136 the satellite observations. The sensitivity of concentrations to emissions is calculated from a
137 trajectory analysis to account for transport of the short-lived gas by using a single CTM forward
138 run. DECSO has been successfully applied to NO₂ observations from OMI and TROPOMI over
139 different regions (Mijling and van der A, 2012; Ding et al., 2017, 2018; van der A et al., 2020).
140 In this study, daily NO_x emissions from January 2019 to April 2020 over East Asia (102–120°E,
141 18–50°N) are derived with DECSO using the Eulerian regional off-line CTM CHIMERE v2013
142 (Menut et al., 2013) and TROPOMI NO₂ observations. The implementation of CHIMERE v2013
143 in DECSO is described in Ding et al. (2015). The latest development and validation of DECSO
144 are presented in previous studies (Ding et al., 2017; van der A et al., 2020). In our current
145 approach, we apply DECSO to the super-observations of TROPOMI instead of directly using
146 individual TROPOMI observations. Figure 1 (c and d) shows the mean NO_x emissions derived
147 from TROPOMI for the same period as Figure 1a and 1b in 2019 and 2020 after the Chinese
148 New Year. We see lower NO_x emissions in February 2020.

149

150 2.3 In-situ observations

151 More than 1500 in-situ stations covering all major cities in China are operated by the
152 China National Environmental Monitoring Centre. They provide hourly observations of the
153 pollutants PM₁₀, PM_{2.5}, O₃, NO₂, SO₂, and CO (Bai et al., 2020). NO₂ is measured by a
154 chemiluminescence technique (Zhang & Zhao, 2015). Data can be accessed via web-sites of
155 third parties, such as www.pm25.in and www.aqicn.org. For this study we have averaged the
156 various in-situ NO₂ observations in a city to a single value per hour for each of 36 selected major
157 cities. For comparison with model results, we calculated a daily value based on the observations
158 from 10:00 to 18:00 local time. The daytime selection is due to large inaccuracies in simulations
159 of the nighttime boundary layer height.

160

161 2.4 Ensemble modelling

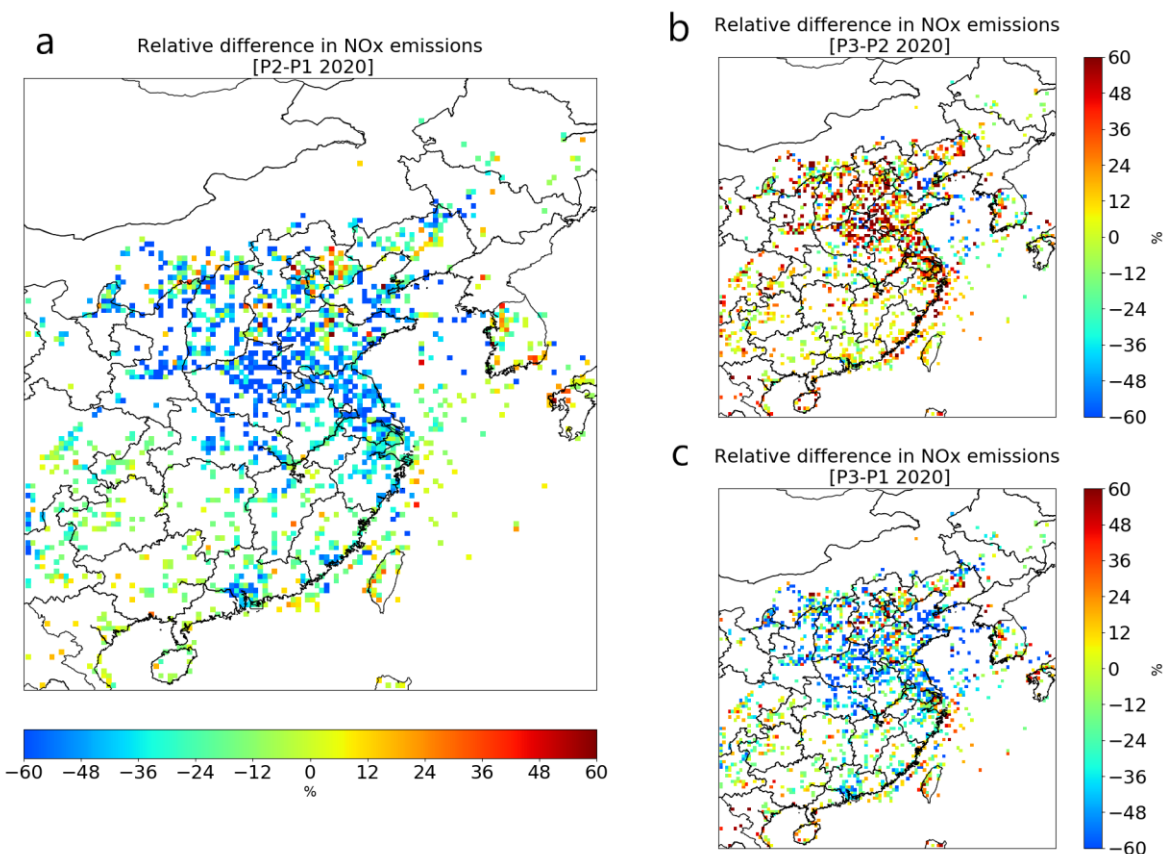
162 An operational multi-model forecasting system for air quality has been developed to
163 provide air quality services for urban areas of China (Brasseur et al., 2019, Petersen et al., 2019).
164 This system has been developed within the EU-funded FP-7 projects: MarcoPolo and PANDA.
165 The ensemble model system includes nine global and regional chemistry-transport models from
166 different research institutes from Europe and China. The ensemble service has a typical
167 resolution of about 20 km. It provides daily forecasts of ozone, nitrogen oxides, and particulate
168 matter for the 36 largest urban areas of East China (i.e. population higher than 3 million
169 according to the census of 2010 (NBS, 2010). These individual 3-day forecasts as well as the
170 mean and median concentrations are publicly accessible (<http://www.marcopolo-panda.eu>). The
171 emission inventories used as input to the models of the ensemble do not account for the Chinese
172 New Year or the COVID-19 lock down period. Therefore, the ensemble model represents the
173 business-as-usual scenario.

174

175 **3 NO_x emissions reductions**

176 NO_x emissions have been affected since the strict regulations started in China, especially
177 in Hubei. We select three periods to quantify the impact of the COVID-19 regulations. The first
178 period (P1) is three weeks before the implementation of the COVID-19 regulations, 3 to 23
179 January in 2020, which is also just before the Chinese New Year. The second period (P2) is 8 to
180 28 February, which is regarded as the regulation period. The third period (P3) is from 18 March
181 to 7 April, when most regions in China resumed working. We calculated the average of NO_x
182 emissions derived with DECSO in each period and compare their differences. Figure 2 shows the
183 relative changes of NO_x emissions during the selected 3 periods over the grid cells with high
184 anthropogenic (above 3kg N/km²/day) NO_x emissions. We observe a strong decrease by at least
185 30% of NO_x emissions over China in P2 compared to P1 (Figure S1 shows the emission changes
186 on provincial level). A few grid cells with increased emissions often coincide with industrial
187 areas. In P3, NO_x emissions increased compared to P2 but are still lower than in P1 because of
188 the step-wise resumption of work and social life. The NO_x emissions in South Korea are not
189 significantly changed in P2 compared to the changes in China during the three periods (Figure
190 S1), because South Korea adopted less restrictive COVID-19 regulations, mostly on voluntary
191 basis (Bauwens et al., 2020). In Figure 2, we see that the NO_x emissions over sea also decrease.
192 We calculate the NO_x emissions over the ship lanes over Chinese seas defined in the study of
193 Ding et al. (2018). The emissions due to sea-transport from Shanghai to Guangzhou are less
194 affected than the transport over land and are found to decrease by about 25% in P2 and increase
195 again with 18% in P3 in comparison to P2. A more significant emission decline was found in the
196 Yellow Sea and Bohai area, where NO_x emissions reduced by about 41% in P2 and continued
197 decreasing by 6% in P3.

198



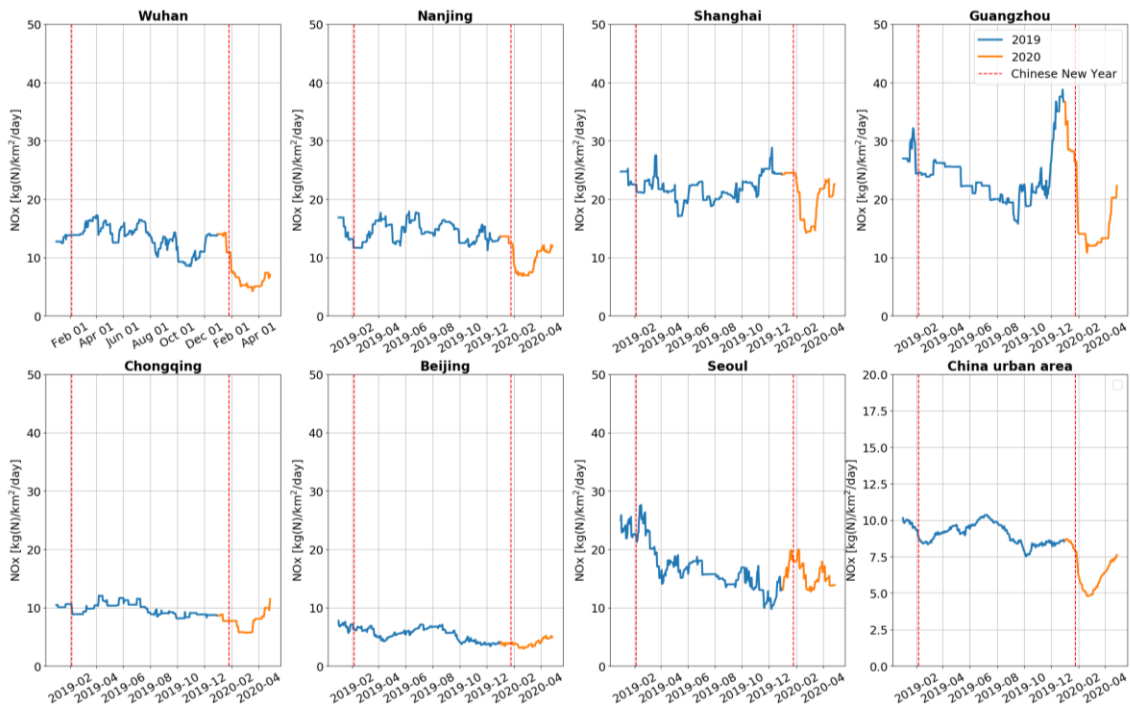
199

200 **Figure 2.** The relative difference in NO_x emissions between (a) P2 and P1; (b) P3 and P2 (c) P3
 201 and P1. P1 is 3-23 January. P2 is 8-28 February. P3 is 18 March to 7 April. The changes in
 202 emissions are shown in the figure for emissions higher than 3 kg(N)/km²/day in P1 to remove
 203 areas with dominating biogenic emissions or rural areas.

204

205 At city level changes in NO_x emissions started from January 2019. Figure 3 shows the
 206 time series of emissions at 6 large cities in China and in Seoul, the capital of South Korea. We
 207 infer a very strong NO_x emission decrease of more than 50% during and after the 2020 Chinese
 208 New Year in Wuhan, where the COVID-19 outbreak was first recorded and very strict lockdown
 209 regulations were adopted. At the other five Chinese cities, we also observe a much stronger
 210 decrease after the Chinese New Year in 2020 than in 2019. In addition, the duration of the period
 211 with low emissions is much longer. Most cities in China display a stronger decrease in 2020 (see
 212 Table S1), which is attributed to the COVID-19 measures. The averaged NO_x emission reduction
 213 at the selected cities shown in table S1 is 35%. We also calculate the average reduction of grid
 214 cells containing urban areas selected by using the land-use data of the GlobCover Land Cover
 215 dataset, which was implemented in the CTM by Ding et al. (2015). The inferred emission
 216 reduction is about 35% in urban areas, which is the same as the average reduction in the selected
 217 cities. Note that the NO_x emissions are usually lower by about 10% during the Chinese New
 218 Year with less business and industrial activities (Ding et al., 2017). The time line of NO_x
 219 emissions in Beijing show a slightly different pattern with a relatively low reduction during the
 220 COVID-19 lockdown, but already strong emission reductions during the politically important

221 “two-sessions” meeting in March 2019, the most important political meeting of China, and
 222 especially the celebration of 70th national anniversary of China around 1 October 2019, when
 223 many factories were closed and strict emission regulations were enforced (Yang et al., 2020).
 224 Figure 3 also shows that the NO_x emissions start to increase again in March, in line with the step-
 225 by-step recovery of the human activities. Except for Wuhan with the emission rebound after 8
 226 April, when the lockdown was lifted, by the end of March all cities reached a level of NO_x
 227 emissions close to what was observed in the same period in 2019. This is consistent with the
 228 economic target of China that they will accelerate the return to the pre-crisis economic level after
 229 the temporary economic setback due to the COVID-19 outbreak as was reported by Ouyang
 230 (2020)
 231



232

233 **Figure 3.** Time series (1 January 2019 to 28 April 2020) of daily NO_x emissions in 7 cities and
 234 urban China. 6 Chinese cities are considered (Wuhan, Nanjing, Shanghai, Guangzhou,
 235 Chongqing and Beijing) as well as Seoul. The location of Chinese cities is shown in Figure S4.

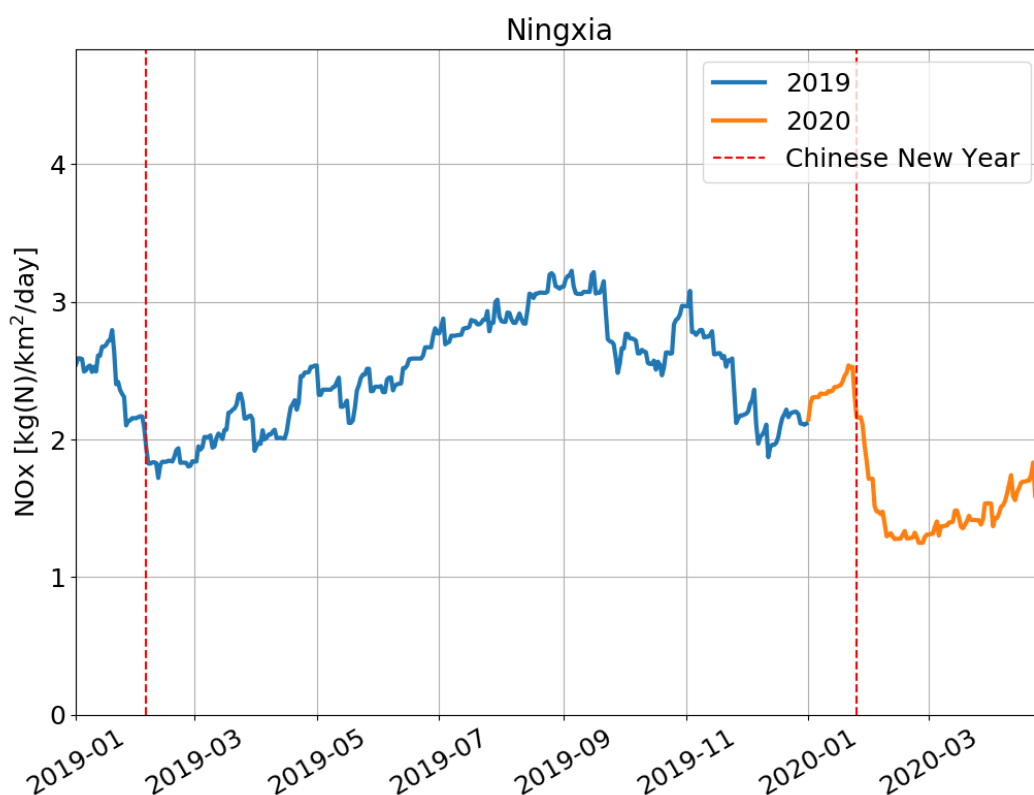
236

237

238 Besides the urban emissions, we find strong reductions of NO_x emissions from coal
 239 power plants. Figure 4 shows time series of NO_x emissions from the Ningxia Province, where the
 240 main sources of NO_x are fossil fuel power plants (van der A et al., 2017). Ningxia province can
 241 serve as an indication of the national energy production by coal power plants. It has a population
 242 of about 6 million, only 0.4% of the total population of China. Its coal production and electricity
 243 generation from coal power plants are in the top ten list of provinces and about 80% of the
 244 generated energy is consumed by the industry (Ningxia Statistics Bureau, 2019). Our inversion

245 results indicate that after the 2020 Chinese New Year, NO_x emissions dropped about 40% in this
 246 province, 20% more than in 2019 New Year period. This shows the impact of the COVID-19
 247 regulations on the energy production, especially in the industrial sector. According to the
 248 National Bureau of Statistics of China (2020), the total profit of the first three months in 2020
 249 made by industrial enterprises decreased around 40% in China compared to the same period of
 250 the previous year. The shrinking of the industrial economy results in lower energy consumption,
 251 which is clearly reflected by the decrease of NO_x emissions from power plants.

252
 253



254
 255 **Figure 4.** Time series (1 January 2019 to 28 April 2020) of daily NO_x emissions in Ningxia
 256 Province.

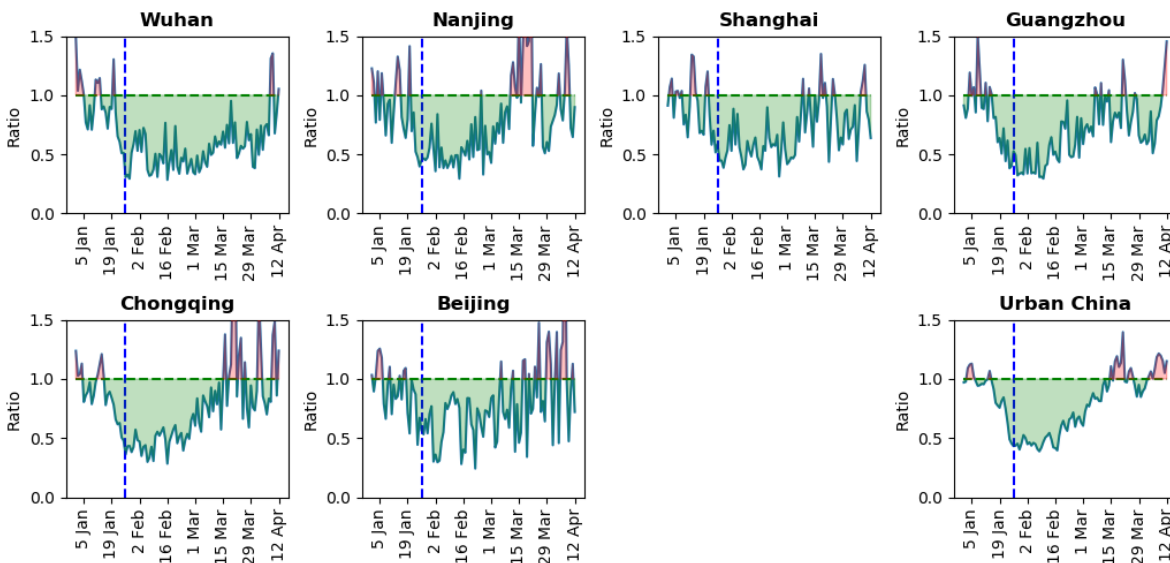
257

258 4 Surface concentration reductions

259 The effect of the emission reductions on the surface concentration is very relevant for air
 260 pollution. In Figure S2 we show the emissions and the modelled surface concentrations from
 261 DECSO based on these emissions. Although we see a similar time course in both, the reductions
 262 in emissions and surface concentrations are different due to the changing meteorology and
 263 lifetime of NO_x over time. To further verify the reductions in surface concentrations we used
 264 measurements of the in-situ stations described in section 2.3. To eliminate the effect of
 265 meteorology and transport we compare the measurements of in-situ stations with the ensemble
 266 model introduced in section 2.4. The model is driven by emission inventories, which are not

267 corrected for the effects of either Spring Festival or the COVID-19 crisis and hence are
 268 considered the business-as-usual situation. A possible bias between measurements and model is
 269 corrected for by normalizing the results for the first two weeks of January. In Figure 5 the ratio
 270 between in-situ measured NO₂ and the modelled NO₂ is shown. The concentration reductions are
 271 shown as green area, while increased concentrations are shown in red. The reduction starts
 272 around the Chinese New Year and ends in March. Exception is the concentration level of Wuhan
 273 that becomes similar to that of the business-as-usual scenario after the first week of April. Table
 274 S1 shows the concentration reduction in P2 compared to P1 for the selected 36 cities. The
 275 average concentration reduction is 41%, while for emissions the reduction is 35%. A striking
 276 difference between Wuhan and the other Chinese cities is the longer duration (by about one
 277 month) of the concentration reductions.

278



279

280 **Figure 5.** Measured NO₂ concentrations (from 1 January to 12 April 2020) compared to
 281 concentrations of the business-as-usual scenario. Cities are chosen similar to Figure 3, except for
 282 Seoul. The Chinese New Year is indicated by the blue dashed line.

283

284 5 Conclusions

285 To study the impact of the COVID-19 regulations on NO_x emissions (one of the key
 286 ingredients determining air pollution), we derived daily NO_x emissions at a resolution of 0.25° ×
 287 0.25° over East Asia from 2019 to March 2020 by applying the inverse algorithm DECSO to
 288 observations from TROPOMI. By grouping the emission into three periods of before, during and
 289 after the COVID-19 regulations, we quantified the emission changes on the small spatial scale of
 290 city level and from different emission sources such as sea-transport and the energy sector. The
 291 observations suggest emission reductions of 20% to 50% for cities. The emissions reduction of
 292 40% in the Ningxia province reflects the impact of the lockdown measures on the energy sector.
 293 Maritime transport is also affected during the COVID-19 regulations, although its emissions
 294 reductions are dependent on the region. Along the ship track from Shanghai to Guangzhou, the
 295 NO_x emissions decreased by 25% during the lockdown and increased again by 18% after the
 296 work resumption. While in the region of the Yellow sea and Bohai sea, the emissions decrease

297 by 40% and continued decreasing with another 6% also in March. To further assess the impact of
298 emission reductions, we compared the in situ NO₂ concentration measurements with simulated
299 surface concentrations from models using unaltered emissions. The emission reductions follow a
300 similar timeline as the surface NO₂ concentrations, which show a sharp reduction around the
301 Chinese New Year and a slow recovery from mid-February to mid-March. Wuhan, the city of the
302 epicenter of the COVID-19 crisis, shows large emission reductions in both February and March,
303 reaching nominal levels in April. In general, we found that activities in the cities returned to
304 normal in March, while as an indicator of the economy, emissions of energy production and
305 international maritime transport, took a longer time to return to pre-COVID-19 levels (Table S2).

306 With the NO_x emissions derived from DECSO using observations from TROPOMI, we
307 are able to get detailed information about the impact on emission changes due to the COVID-19
308 regulations by accounting for the influence of meteorology, lifetime and transport of the air
309 pollutants. As the COVID-19 crisis progressively affects all continents, the public health
310 regulations implemented by various countries may have different contributions to air quality.
311 Applying our methodology to different regions can help to quantify the impact of the NO_x
312 emission reductions by the different regulations on not only the improvement of air quality from
313 urban to local to regional scale.

314 **Acknowledgments and Data**

315 This research has been supported by the project “Impact study of COVID-19 lockdown
316 measures on air quality and climate” of the European Space Agency (grant number
317 4000127610/19/I-NS). This publication contains modified Copernicus Sentinel-5P data 2019-
318 2020. TROPOMI data are available at
319 http://www.temis.nl/airpollution/no2col/tropomi_data.php. We acknowledge the ESA
320 GlobCover project for the land use data set on http://due.esrin.esa.int/page_globcover.php. The
321 NO_x emissions dataset in this study is available on
322 http://www.globemission.eu/region_asia/datapage.php?species=NOx_TROPOMI.
323

324 **References**

325 Bai, K., Li, K, Guo, J., Yang, Y., Chang, N.-B. (2020). Filling the gaps of in situ hourly PM_{2.5}
326 concentration data with the aid of empirical orthogonal function analysis constrained by diurnal
327 cycles. *Atmospheric Measurement Techniques*, 13, 3, 1213-1226, DOI: 10.5194/amt-13-1213-
328 2020.

329
330 Bauwens, M., Compernelle, S., Stavrakou, T., Müller, J.-F., van Gent, J., Eskes, H., et al. (2020).
331 Impact of coronavirus outbreak on NO₂ pollution assessed using TROPOMI and OMI
332 observations. *Geophysical Research Letters*, <https://doi.org/10.1029/2020GL087978>, 2020

333
334 Boersma, K. F., Vinken, G. C. M., & Eskes, H. J. (2016). Representativeness errors in comparing
335 chemistry transport and chemistry climate models with satellite UV–Vis tropospheric column
336 retrievals. *Geosci. Model Dev.*, 9(2), 875-898. doi:10.5194/gmd-9-875-2016

337

- 338 Brasseur, G. P., Xie, Y., Petersen, A. K., Bouarar, I., Flemming, J., Gauss, M., et al. (2019).
339 Ensemble forecasts of air quality in eastern China - Part 1: Model description and
340 implementation of the MarcoPolo-Panda prediction system, version 1, *Geosci. Model Dev.*, 12,
341 33-67, <https://doi.org/10.5194/gmd-12-33-2019>.
- 342
- 343 Ding, J., van der A, R. J., Mijling, B., Levelt, P. F., & Hao, N. (2015). NO_x emission estimates
344 during the 2014 Youth Olympic Games in Nanjing. *Atmos. Chem. Phys.*, 15(16), 9399-9412.
345 doi:10.5194/acp-15-9399-2015
- 346
- 347 Ding, J., Miyazaki, K., van der A, R. J., Mijling, B., Kurokawa, J. I., et al. (2017).
348 Intercomparison of NO_x emission inventories over East Asia. *Atmos. Chem. Phys.*, 17(16),
349 10125-10141. doi:10.5194/acp-17-10125-2017
- 350
- 351 Ding, J., A, R. J., Mijling, B., Jalkanen, J. P., Johansson, L., & Levelt, P. F. (2018). Maritime
352 NO_x Emissions Over Chinese Seas Derived From Satellite Observations. *Geophysical Research*
353 *Letters*, 45(4), 2031-2037. doi:doi:10.1002/2017GL076788
- 354 Goldberg, D., L., Lu, Z., Streets, D., G., de Foy, B., Griffin, D., McLinden, C., A., et al. (2019).
355 Enhanced Capabilities of TROPOMI NO₂: Estimating NO_x from North American Cities and
356 Power Plants, *Environ. Sci. Technol.*, 53, 21, 12594-12601,
357 <https://doi.org/10.1021/acs.est.9b04488>.
- 358
- 359 Gu, J., Chen, L., Yu, C., Li, S., Tao, J., Fan, M., et al. (2017) Ground-Level NO₂ Concentrations
360 over China Inferred from the Satellite OMI and CMAQ Model Simulations. *Remote Sens.*, 9(6),
361 519, <https://doi.org/10.3390/rs9060519>
- 362
- 363 Huang, X., Ding, A., Gao, J., Zheng, B., Zhou, D., et al. (2020). Enhanced secondary pollution
364 offset reduction of primary emissions during COVID-19 lockdown in China. *EarthArXiv.*, April
365 13. <https://doi.org/10.31223/osf.io/hvuzy>
- 366
- 367 Judd, L. M., Al-Saadi, J. A., Szykman, J. J., Valin, L. C., Janz, S. J., Kowalewski, M. G., et al.
368 (2020). Evaluating Sentinel-5P TROPOMI tropospheric NO₂ column densities with airborne and
369 Pandora spectrometers near New York City and Long Island Sound. *Atmos. Meas. Tech.*
370 *Discuss.*, 2020, 1-52. doi:10.5194/amt-2020-151
- 371 Liu, F., Page, A., Strode, S. A., Yoshida, Y., Choi, S., Zheng, B., et al. (2020). Abrupt decline in
372 tropospheric nitrogen dioxide over China after the outbreak of COVID-19. *Science Advances*,
373 eabc2992. doi:10.1126/sciadv.abc2992
- 374
- 375 Menut, L., Bessagnet, B., Khvorostyanov, D., Beekmann, M., Blond, N., Colette, A., et al.
376 (2013). CHIMERE 2013: A model for regional atmospheric composition modelling.
377 *Geoscientific Model Development*, 6(4), 981–1028. <https://doi.org/10.5194/gmd-6-981-2013>

- 378
- 379 Mijling, B., and van der A, R. J. (2012). Using daily satellite observations to estimate emissions
380 of short-lived air pollutants on a mesoscopic scale. *Journal of Geophysical Research:*
381 *Atmospheres*, 117(D17). doi:10.1029/2012JD017817
- 382
- 383 Miyazaki, K., Eskes, H. J., & Sudo, K. (2012). Global NO_x emission estimates derived from an
384 assimilation of OMI tropospheric NO₂ columns. *Atmospheric Chemistry and Physics*, 12(5),
385 2263-2288. doi:10.5194/acp-12-2263-2012
- 386
- 387 Miyazaki, K., Bowman, K., Sekiya, T., Eskes, H., Boersma, F., Worden, H., et al. (2020). An
388 updated tropospheric chemistry reanalysis and emission estimates, TCR-2, for 2005–2018, *Earth*
389 *Syst. Sci. Data Discuss.*, <https://doi.org/10.5194/essd-2020-30>, in review.
- 390
- 391 National Bureau of Statistics of China (2020). Available online:
392 http://www.stats.gov.cn/english/PressRelease/202004/t20200428_1742015.html (last access
393 date: 3 May 2020)
- 394
- 395 NBS, National Bureau of Statistics, China Statistical Yearbook 2010 ,Beijing: China Statistics
396 Press, 2010
- 397
- 398 Ningxia Statistics Bureau (2019). The Achievements of Economic and Social Development
399 during the last 70 years, part 3, in Chinese. Available online:
400 http://tj.nx.gov.cn/tjxx/201909/t20190923_1750612.html (last access date: 9 May 2020)
- 401
- 402 Ouyang S. (2020). COVID-19 will not alter China's growth story, top economic regulator says,
403 *China Daily*. Available online:
404 <https://global.chinadaily.com.cn/a/202004/20/WS5e9d51f8a3105d50a3d1779c.html> (last access
405 date: 27 April 2020)
- 406
- 407 Petersen, A. K., Brasseur, G. P., Bouarar, I., Flemming, J., Gauss, M., Jiang, F., et al (2019).
408 Ensemble forecasts of air quality in eastern China - Part 2: Evaluation of the MarcoPolo-Panda
409 prediction system, version 1. *Geosci. Model Dev.*, 12, 1241-1266, [https://doi.org/10.5194/gmd-](https://doi.org/10.5194/gmd-12-1241-2019)
410 12-1241-2019.
- 411
- 412 Shindell, D. T., Faluvegi, G., Koch, D. M., Schmidt, G. A., Unger, N., & Bauer, S. E. (2009).
413 Improved Attribution of Climate Forcing to Emissions. *Science*. 326(5953), 716-718.
414 doi:10.1126/science.1174760
- 415

416 Stavrakou, T., Müller, J.-F., Boersma, K. F., van der A, R. J., Kurokawa, J., Ohara, T., and
417 Zhang, Q. (2013). Key chemical NO_x sink uncertainties and how they influence top-down
418 emissions of nitrogen oxides, *Atmos. Chem. Phys.*, 13, 9057–9082, [https://doi.org/10.5194/acp-](https://doi.org/10.5194/acp-13-9057-2013)
419 13-9057-2013,.

420

421 Tack, F., Merlaud, A., Iordache, M. D., Pinardi, G., Dimitropoulou, E., Eskes, H., et al. (2020).
422 Assessment of the TROPOMI tropospheric NO₂ product based on airborne APEX observations.
423 *Atmos. Meas. Tech. Discuss.*, 2020, 1-55. doi:10.5194/amt-2020-148

424

425 Tian, H., Liu, Y., Li, Y., Wu, C.-H., Chen, B., Kraemer, M. U. G., et al. (2020). An investigation
426 of transmission control measures during the first 50 days of the COVID-19 epidemic in China.
427 *Science*, eabb6105. doi:10.1126/science.abb6105

428

429 van der A, R. J., Mijling, B., Ding, J., Koukouli, M. E., Liu, F., Li, Q., et al. (2017). Cleaning up
430 the air: effectiveness of air quality policy for SO₂ and NO_x emissions in China. *Atmos. Chem.*
431 *Phys.*, 17(3), 1775-1789. doi:10.5194/acp-17-1775-2017

432

433 van der A, R. J., de Laat, A. T. J., Ding, J., & Eskes, H. J. (2020). Connecting the dots: NO_x
434 emissions along a West Siberian natural gas pipeline. *npj Climate and Atmospheric Science*,
435 3(1), 16. doi:10.1038/s41612-020-0119-z

436

437 van Geffen, J., Boersma, K. F., Eskes, H., Sneep, M., ter Linden, M., Zara, M., and Veefkind, J.
438 P.: S5P TROPOMI NO₂ slant column retrieval: method, stability, uncertainties and comparisons
439 with OMI, *Atmos. Meas. Tech.*, 13, 1315–1335, [https://doi.org/10.5194/amt-](https://doi.org/10.5194/amt-13-1315-2020)
440 13-1315-2020.

441

442 van Geffen, J. H. G. M., Eskes, H. J., Boersma, K. F., Maasackers, J. D., and Veefkind, J. P.
443 (2019). TROPOMI ATBD of the total and tropospheric NO₂ data products, Report S5P-KNMI-
444 L2-0005-RP, version 1.4.0, released 6 February 2019, KNMI, De Bilt, the Netherlands, available
445 at: <http://www.tropomi.eu/documents/atbd/>, last access: 17 March 2020.

446

447 Veefkind, J. P., Aben, I., McMullan, K., Förster, H., de Vries, J., Otter, G., et al. (2012).
448 TROPOMI on the ESA Sentinel-5 Precursor: A GMES mission for global observations of the
449 atmospheric composition for climate, air quality and ozone layer applications. *Remote Sensing of*
450 *Environment*, 120, 70-83. doi:<https://doi.org/10.1016/j.rse.2011.09.027>

451

452 Verhoelst, T., Compernelle, S., Pinardi, G., Lambert, J. C., Eskes, H. J., Eichmann, K. U., et al.
453 (2020). Ground-based validation of the Copernicus Sentinel-5p TROPOMI NO₂ measurements
454 with the NDACC ZSL-DOAS, MAX-DOAS and Pandonia global networks. *Atmos. Meas. Tech.*
455 *Discuss.*, 2020, 1-40. doi:10.5194/amt-2020-119

456

457 Wang, P., Chen, K., Zhu, S., Wang, P., & Zhang, H. (2020). Severe air pollution events not
458 avoided by reduced anthropogenic activities during COVID-19 outbreak. *Resources,*
459 *Conservation and Recycling*, 158, 104814. doi:<https://doi.org/10.1016/j.resconrec.2020.104814>

460

461 WHO (2020). The World Health Organization. Coronavirus Disease (COVID-19) Pandemic.
462 Available online: <https://www.who.int/emergencies/diseases/novel-coronavirus-2019> (last access
463 date: 27 April 2020)

464

465 Yang, Y., Wang, Y., Yao, D., Zhao, S., Yang, S., et al. (2020). Significant decreases in the
466 volatile organic compound concentration, atmospheric oxidation capacity and photochemical
467 reactivity during the National Day holiday over a suburban site in the North China Plain,
468 *Environmental Pollution*, Volume 263, Part A, 114657,
469 <https://doi.org/10.1016/j.envpol.2020.114657>.

470

471 Zhang, R., Zhang, Y., Lin, H., Feng, X., Fu, T.-M., & Wang, Y. (2020). NO_x Emission
472 Reduction and Recovery during COVID-19 in East China. *Atmosphere*, 11(4), 433

473

474 Zhang, Y., Cao, F. (2015) Fine particulate matter (PM_{2.5}) in China at a city level. *Sci Rep* 5,
475 14884. <https://doi.org/10.1038/srep14884>

476

477

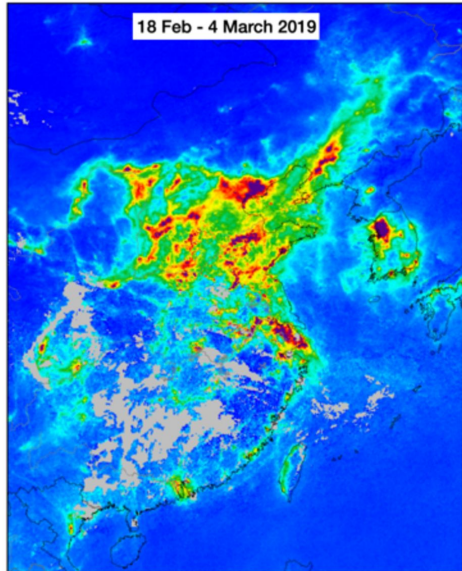
478

479

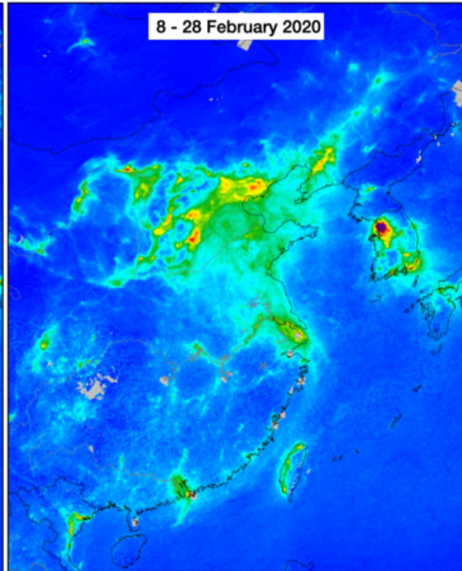
480

Figure 1.

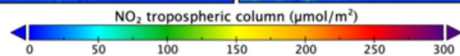
18 Feb - 4 March 2019



8 - 28 February 2020

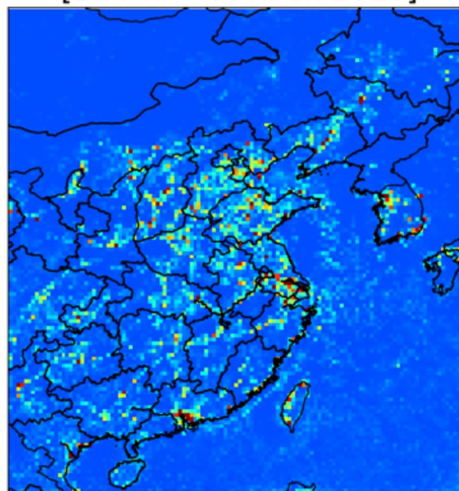


a

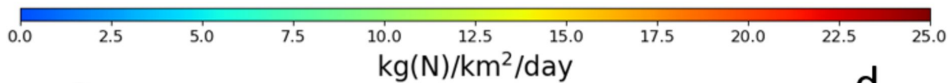
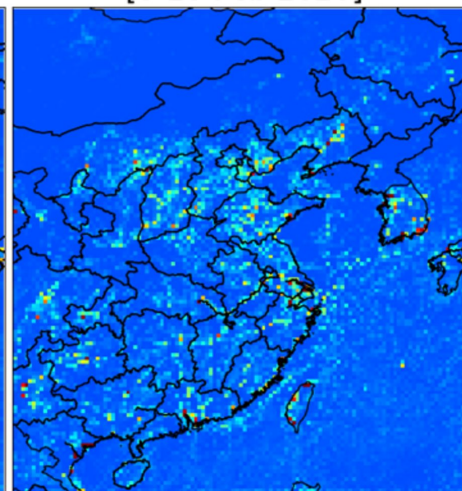


b

NOx emissions
[18 Feb - 4 March 2019]



NOx emissions
[8-28 Feb 2020]

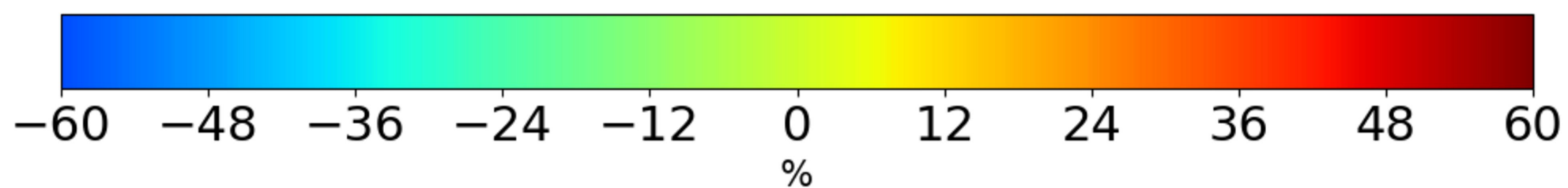
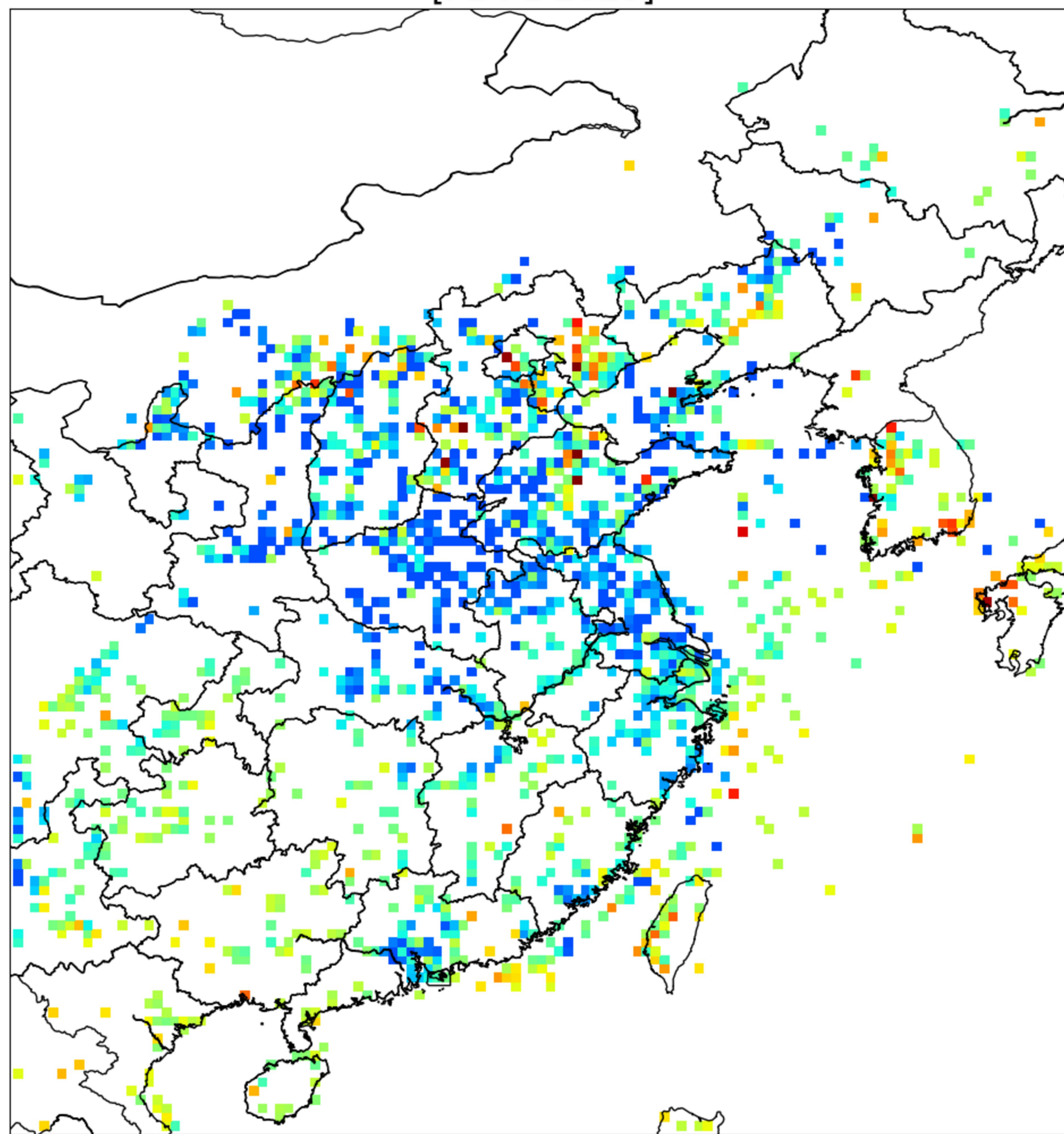


c

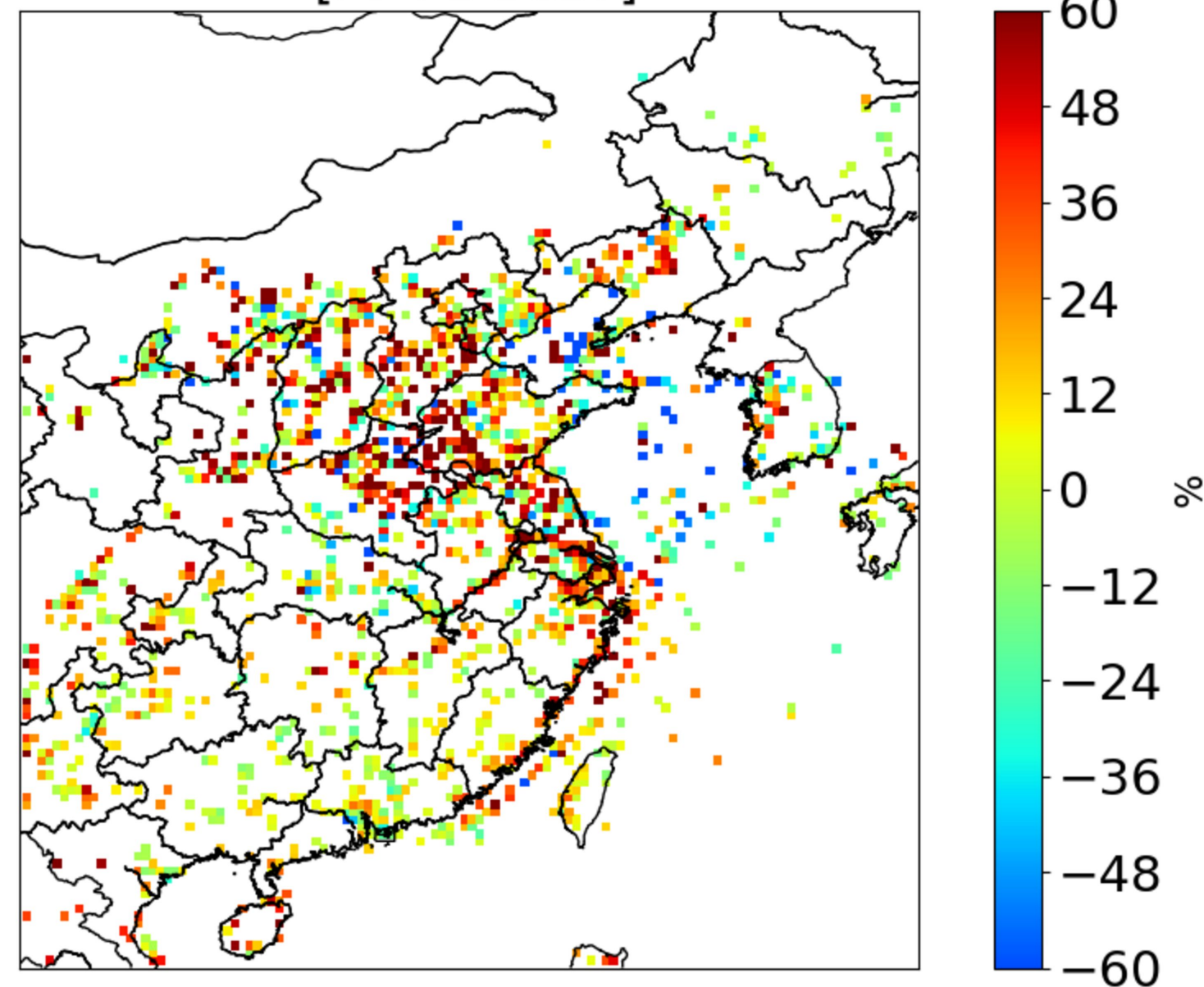
d

Figure 2.

a Relative difference in NO_x emissions
[P2-P1 2020]



b Relative difference in NO_x emissions
[P3-P2 2020]



c Relative difference in NO_x emissions
[P3-P1 2020]

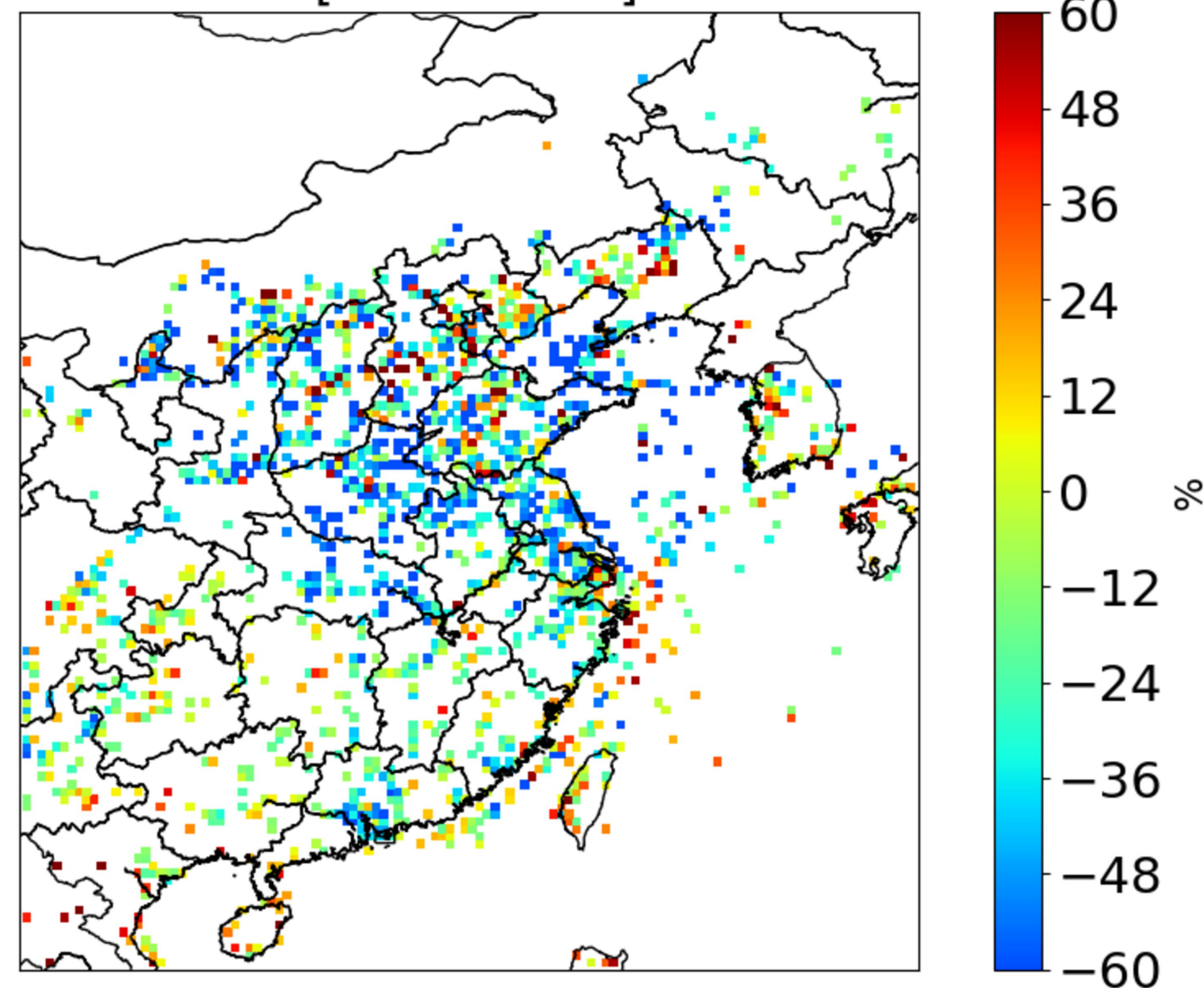


Figure 3.

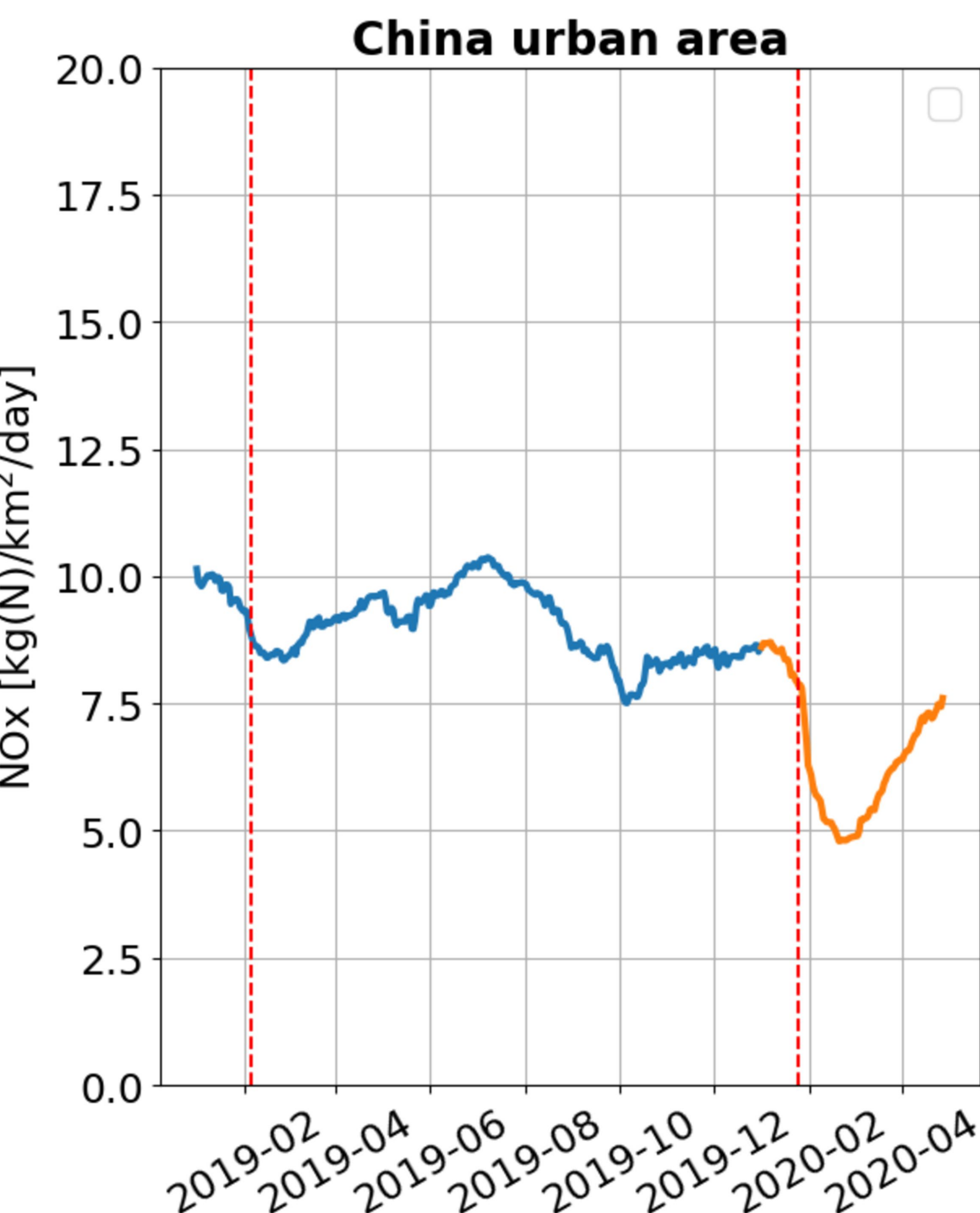
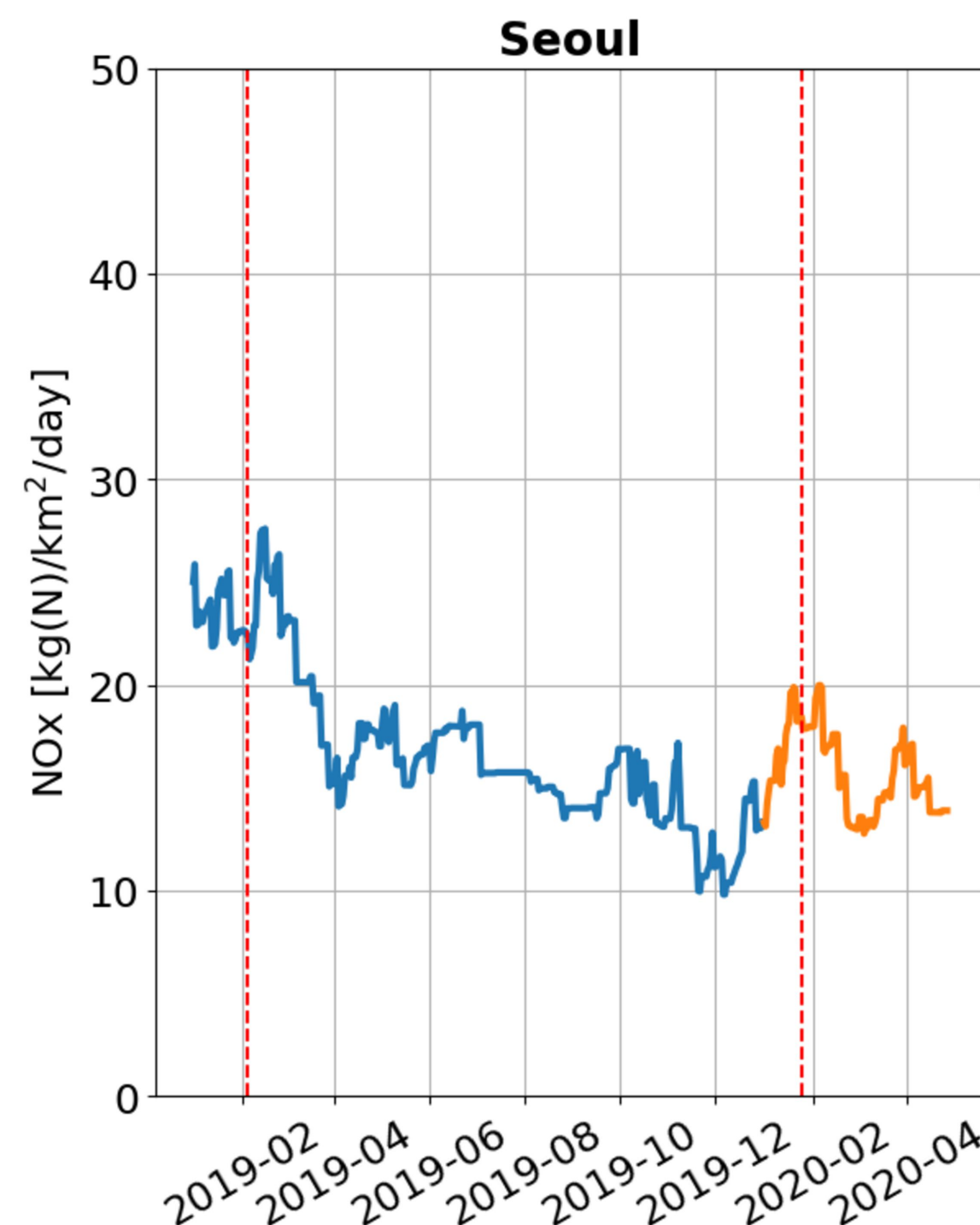
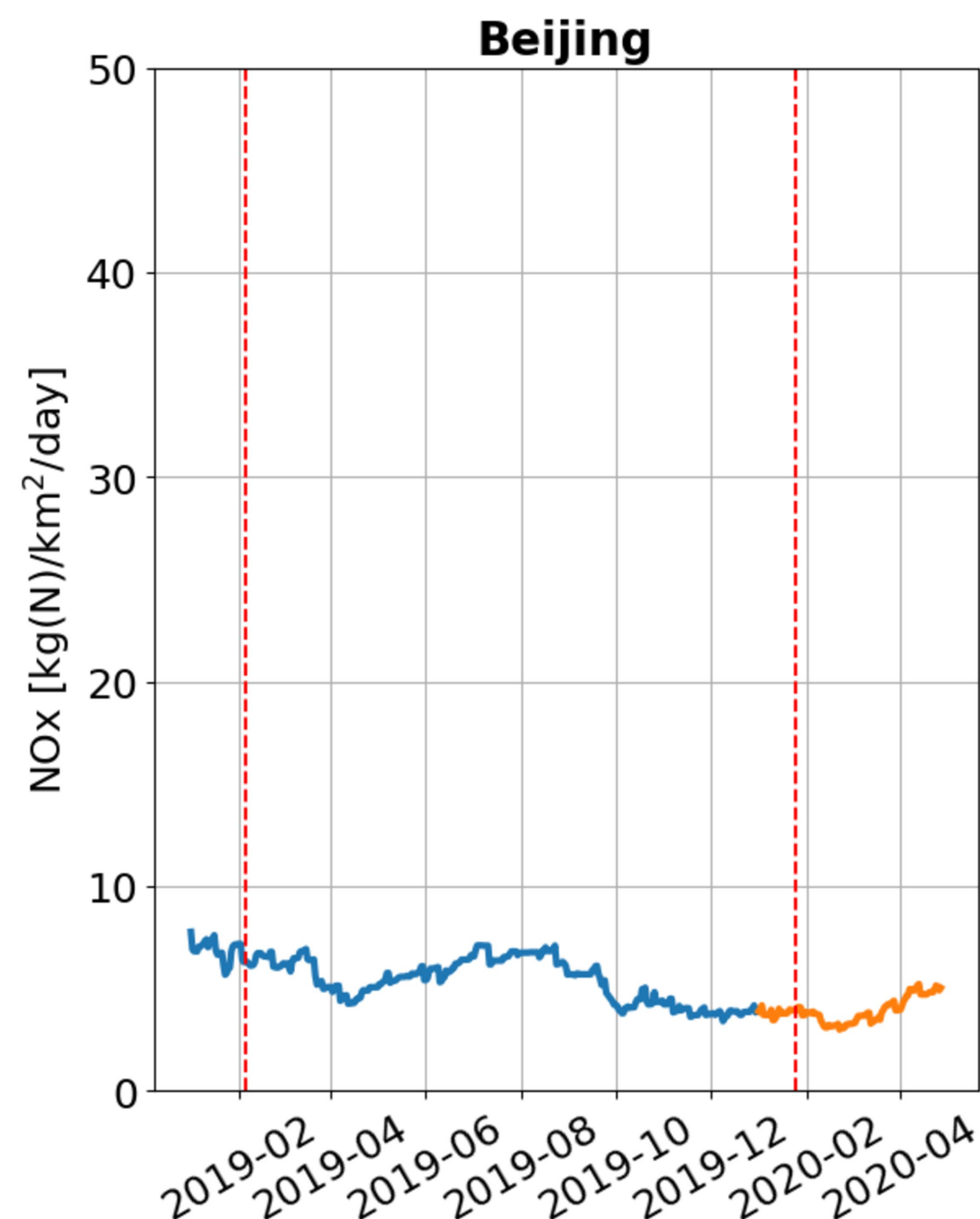
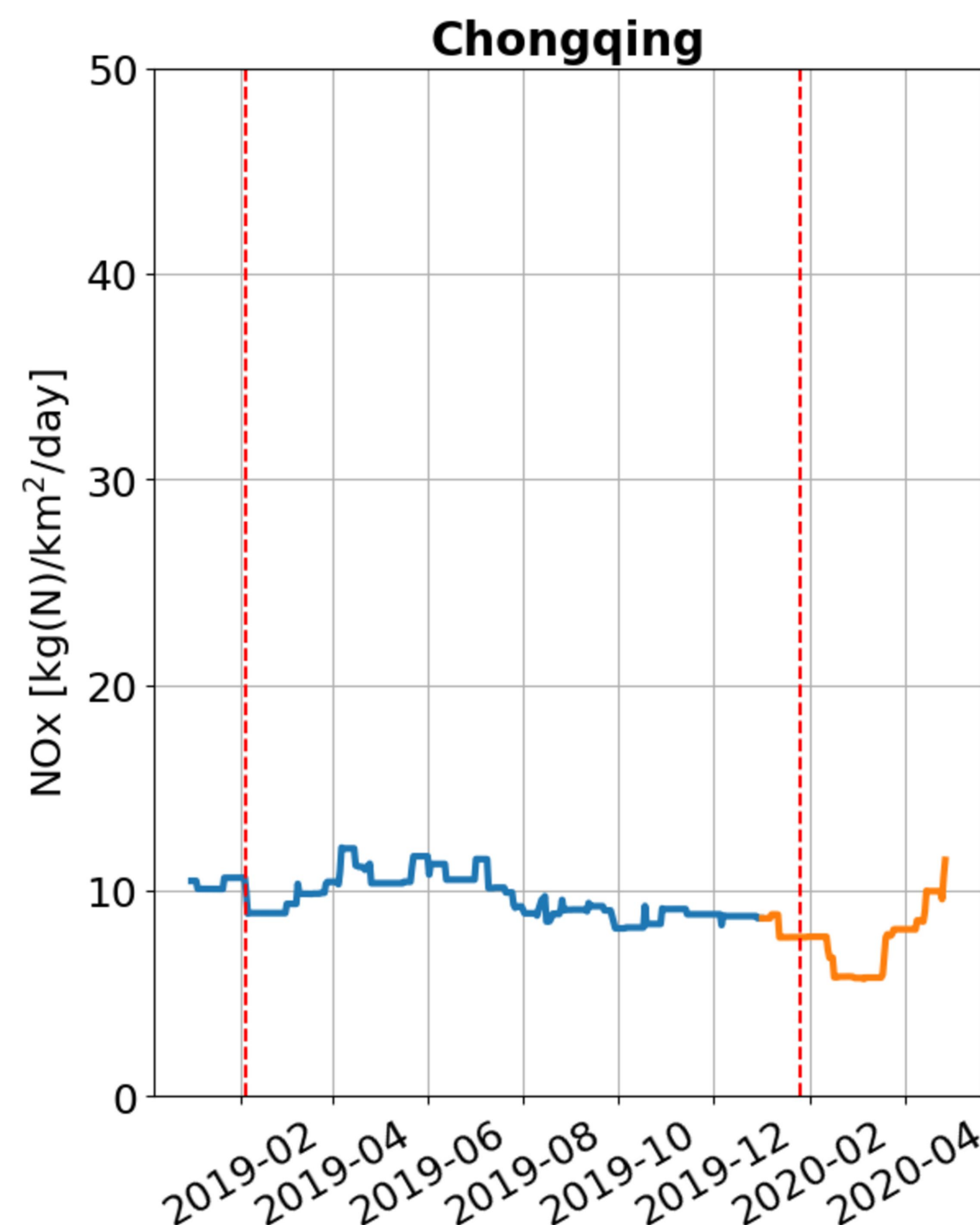
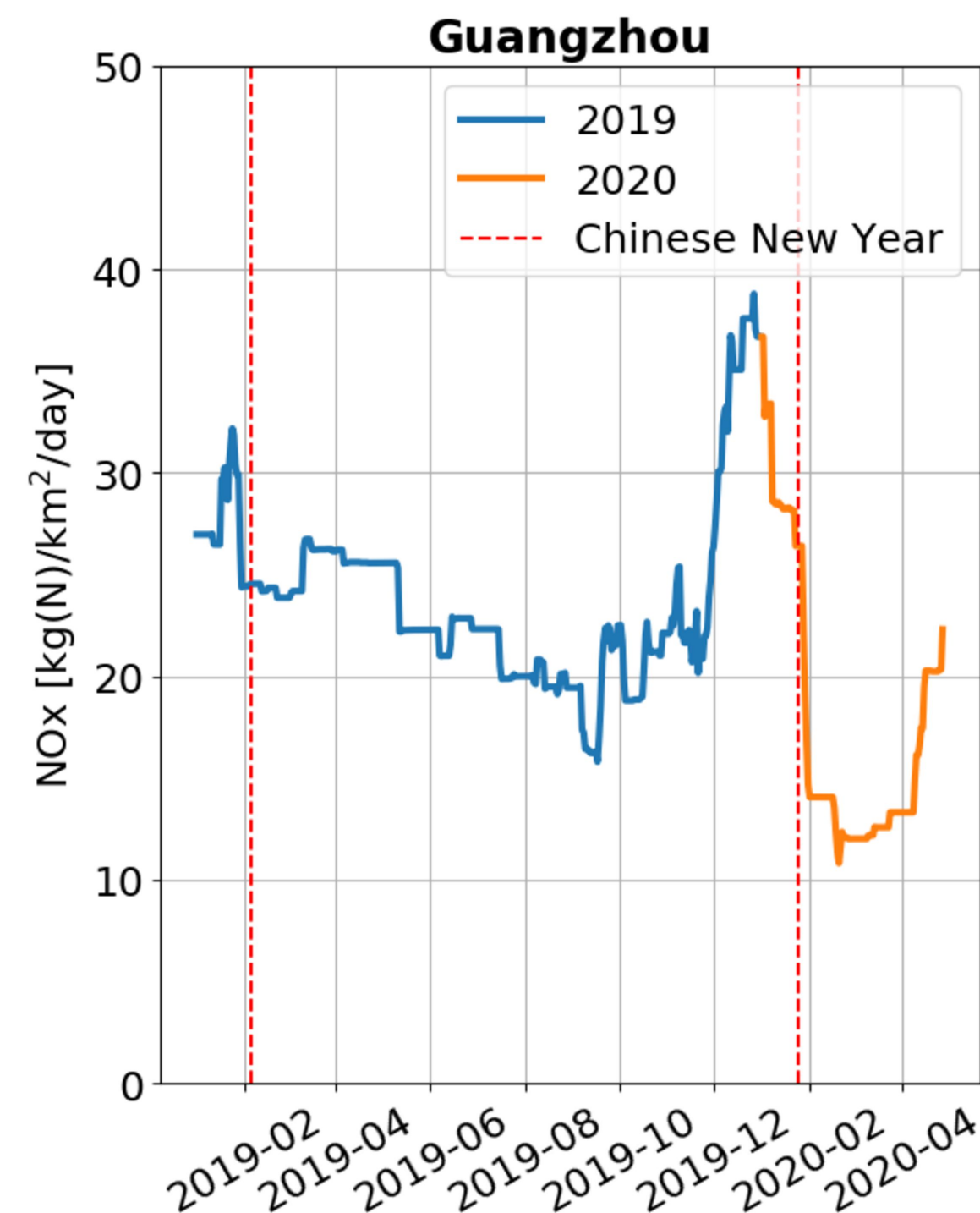
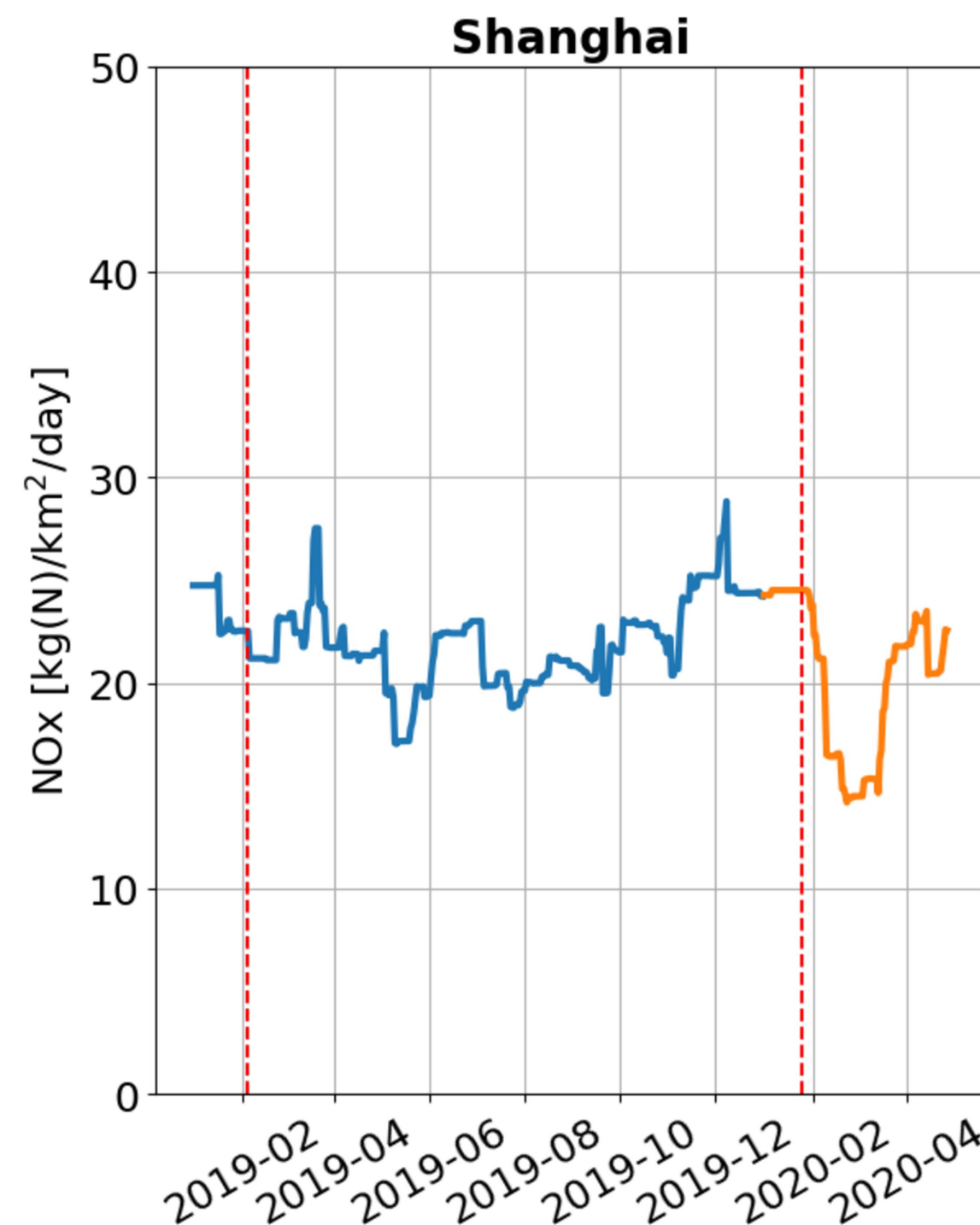
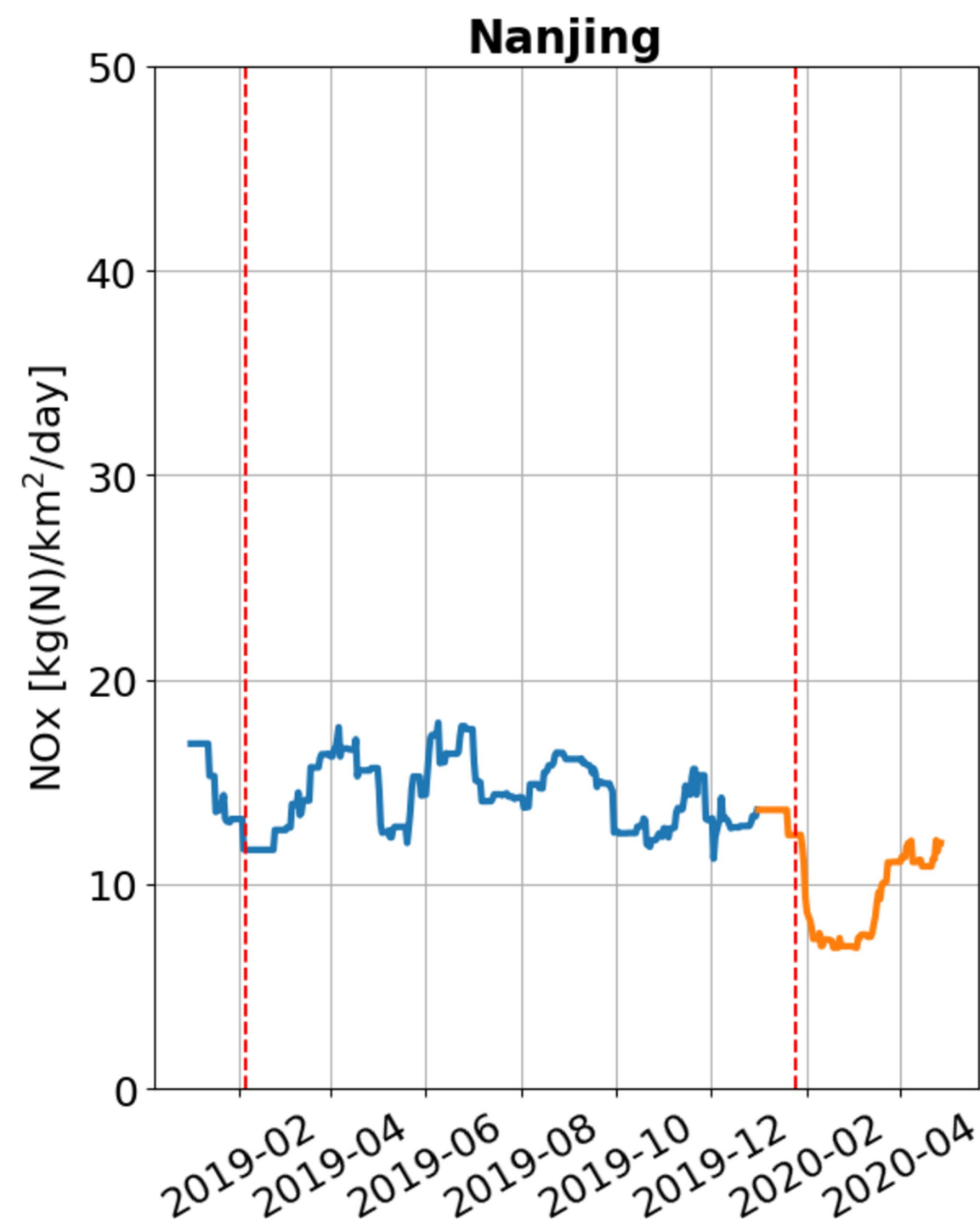
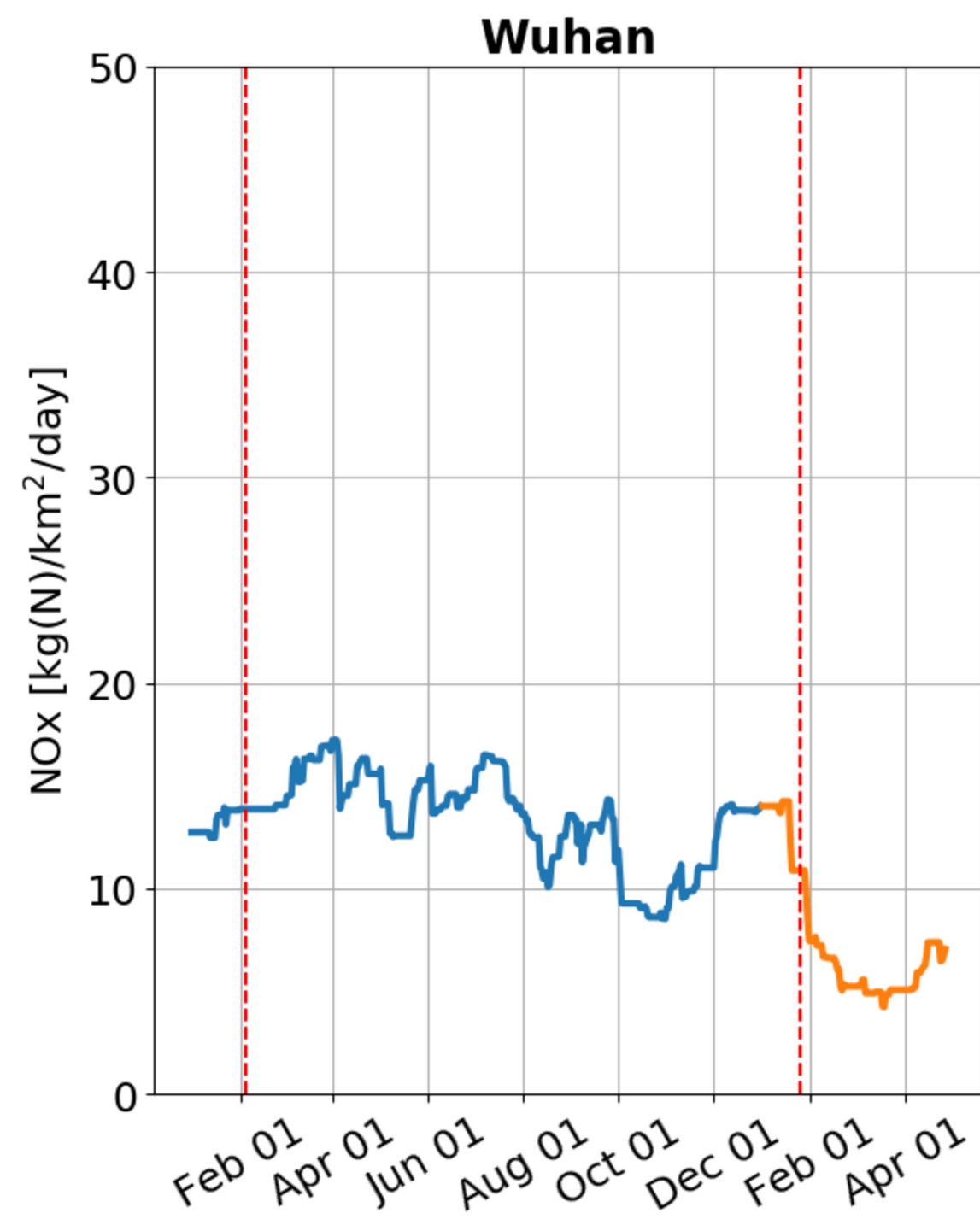


Figure 4.

Ningxia

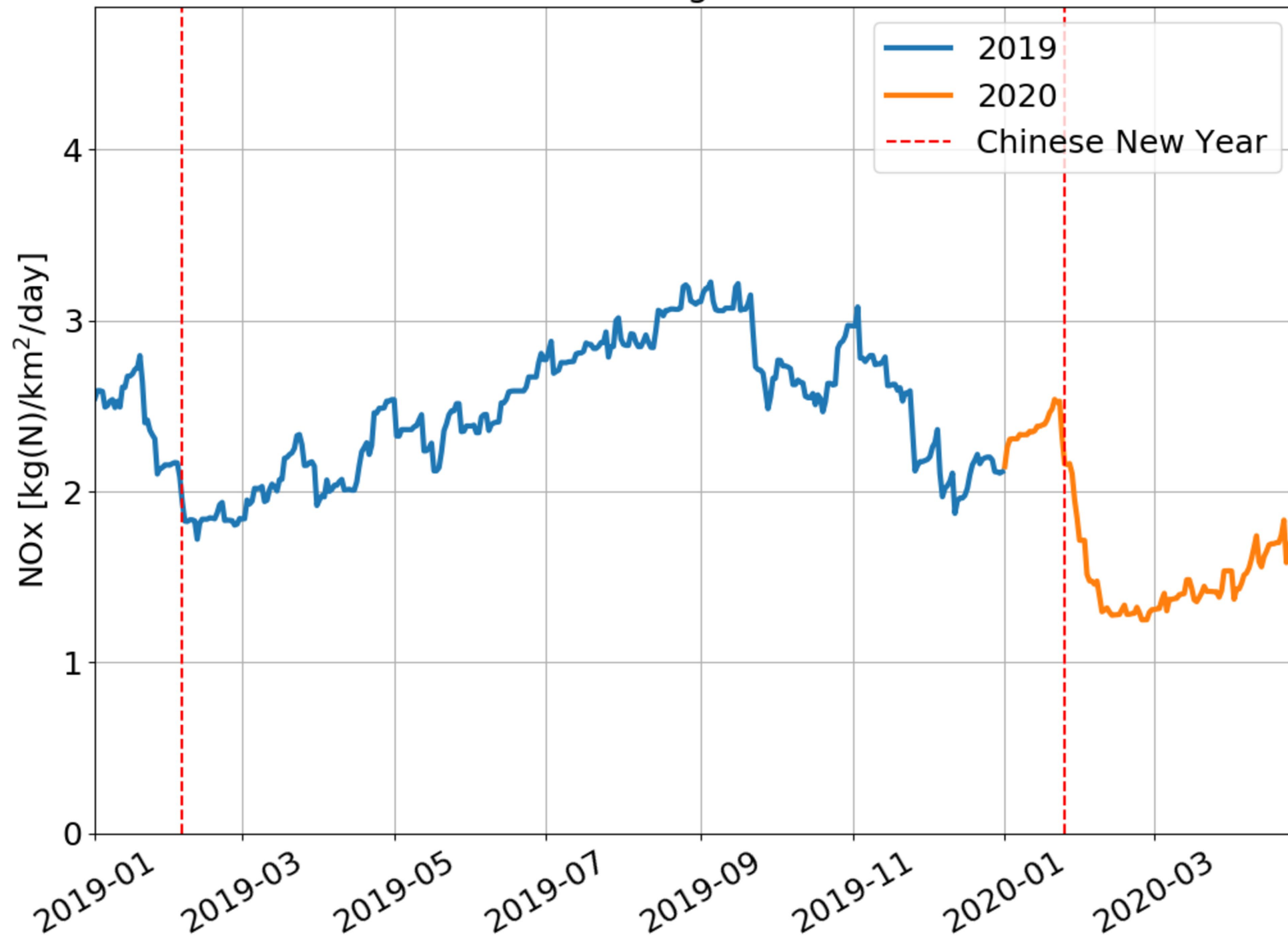
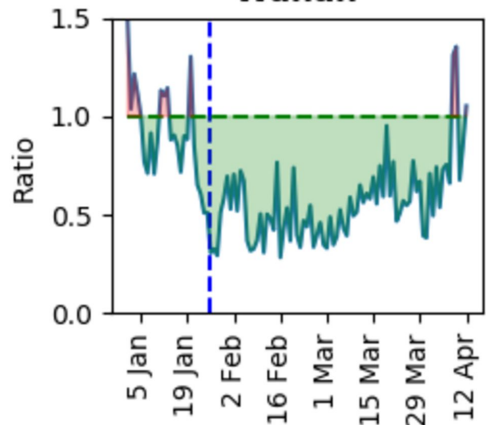
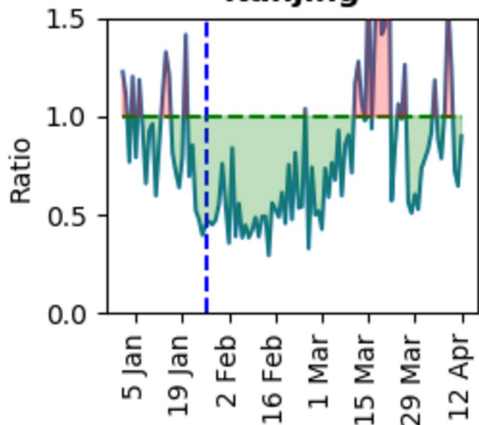
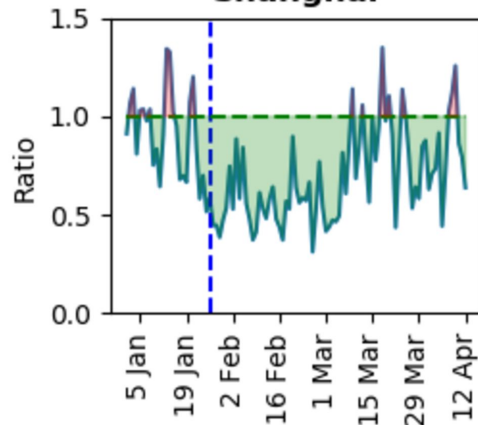
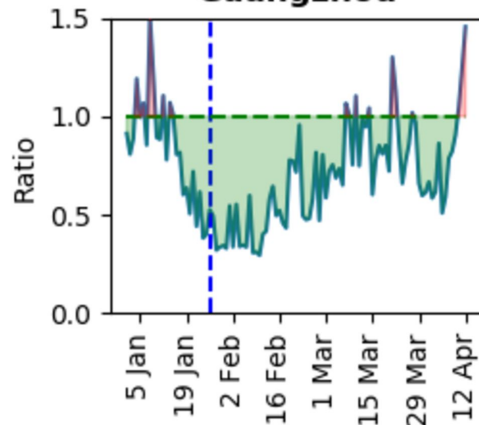
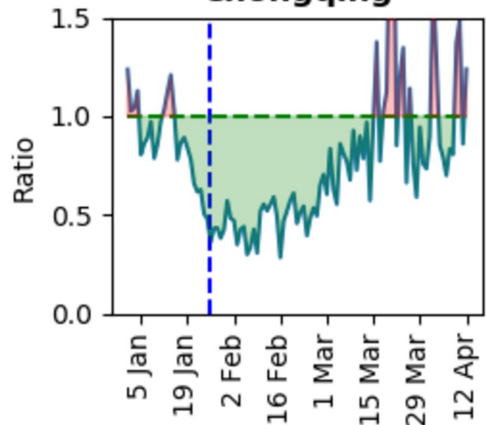
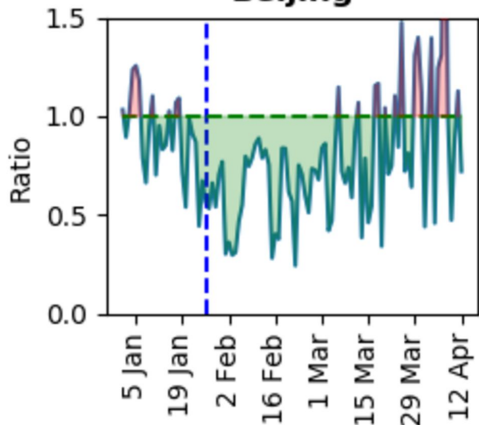


Figure 5.

Wuhan**Nanjing****Shanghai****Guangzhou****Chongqing****Beijing****Urban China**